


# POVM actuele sterkte

Parameter assessment

Activiteit 4: Toepassen beter berekeningsmodel  
EEM

POV

MACRO  
STABILITEIT



Auteur: M. Konstantinou

Datum: jan. 2017

Versie: 1




**Project**  
1220518-004

**Pagina's**  
51

**Samenvatting**

For the POVM project Actuele Sterkte a comprehensive laboratory study is conducted. This report discusses the results and reports the parameter assessment for the parameters to be used in the actual stability assessment. The calculation results will be presented in a companion report.

The actuele sterkte project focusses on 4 cross sections of the dike along the river Hollandse IJssel. The tested samples were retrieved at those cross sections. The laboratory testing program consists of DSS, CAU, Ko-CRS and LDSS tests on clay and peat samples. The tests were performed by Deltares in co-operation with Wiertsema and Partners. The parameters are determined to be used in LEM as well as in FEM calculations.

Versie	Datum	Auteur	Paraaf Review	Paraaf Goedkeuring	Paraaf
	Jan. 2017	M. Konstantinou PhD	 Dr.ir. C. Zwaneburg	 Ir. L. Voogt	

**Status**  
Definitief

9 februari 2017, definitief

## Inhoud

<b>1</b>	<b>Introduction</b>	<b>1</b>
1.1	Background	1
1.2	Goal of report	3
1.3	Strategy	3
<b>2</b>	<b>Geotechnical laboratory test results</b>	<b>5</b>
2.1	Laboratory testing plan	5
2.2	Static triaxial tests	5
2.3	Direct simple shear tests	6
2.4	Ko-CRS tests	8
2.5	Large DSS tests, LDSS	8
2.6	Index laboratory tests	9
<b>3</b>	<b>Soil parameter assessment</b>	<b>11</b>
3.1	Geotechnical laboratory test results	11
3.1.1	General	11
3.1.2	Assessment of undrained shear strength	11
3.1.3	Assessment of shear strength ratio	13
3.1.4	Assessment of stiffness parameters	17
3.1.5	Assessment of drained shear strength parameters	22
3.1.6	Assessment of undrained Young's Modulus, E and shear modulus, G	26
3.1.7	LDSS test results	34
3.2	In situ test results	41
3.2.1	General	41
3.2.2	Assessment of undrained shear strength	41
3.2.3	Assessment of yield stress	44
3.3	Comparison with data from previous soil investigation campaign (KIJK Project)	46
<b>4</b>	<b>Summary and Conclusions</b>	<b>49</b>
<b>5</b>	<b>References</b>	<b>51</b>
<b>Appendices</b>		
<b>A</b>	<b>Geological profile of cross sections</b>	<b>A-1</b>
<b>B</b>	<b>Computation of field effective stress level</b>	<b>B-1</b>
<b>C</b>	<b>CAU test results</b>	<b>C-1</b>
<b>D</b>	<b>DSS test results</b>	<b>D-1</b>
<b>E</b>	<b>K<sub>o</sub>-CRS results</b>	<b>E-1</b>



*9 februari 2017, definitief*

<b>F Large DSS results</b>	<b>F-1</b>
<b>G Atterberg limit results</b>	<b>G-1</b>
<b>H PSD test results</b>	<b>H-1</b>
<b>I Classification test results</b>	<b>I-1</b>

# 1 Introduction

## 1.1 Background

The aim of the POVM programme (Project Overstijgende Verkenning Macrostablieiteit) is to support new methods and processes in dike improvement and where needed, to develop this further. An important aspect in the design of a dike improvement is to account for uncertainties in strength- parameters of the dike body and the subsoil. Within the POVM-programme the research project Actuele Sterkte, POVM-AS, is defined which deals with this aspect.

Specifically, the research goal of the POVM is to develop calculation methods and tools in combination with specific monitoring, in order to reduce the uncertainty in design. This is of benefit, as it might reduce the number of dike sections that need improvement or the measures of dike improvement can be more economical.

Additionally, more insight can be gained by considering the past performance of the considered dike sections during relevant loading conditions. This requires the development for new methods that account for observations in the past.

Some dike sections that are part of the dike improvement programme HWBP, have faced more severe loading conditions than the present design load. Still, calculations show that these sections do not meet the required safety levels. These observations might indicate that the uncertainties in the design parameters lead to a highly conservative design, i.e. some of the parameter relations need adjustment. Furthermore, the survival under loads that are close to the critical design loads might contribute to more certainty in the real strength of these dikes.

In near future, the new requirements for dike design will be based on the risk of flooding, instead of on the chance of exceeding a critical water level. In addition, the material behaviour in the slope stability calculations will be treated as 'undrained', for cohesive material, below the phreatic line. This is a better approach of the material behaviour in slope stability, than the traditional Dutch partially drained method.

The strength of dikes can be determined more accurately by using (improved) calculation methods that are currently under development, in combination with monitoring of pore water pressure and other specific field and laboratory research. These insights are more specific than what is prescribed in general, and dike sections that were considered to be 'unsafe' might deemed to be 'safe' by using these insights (reduction of scope) or the dimensions of the dike reinforcement can be reduced.

The impact of the new calculation methods will be demonstrated for several cases in the Hollandse IJssel dike in the Krimpenerwaard. A large part of these cases is located in the region of the dike strengthening project KIJK (Krachtige IJsseldijken Krimpenerwaard), in which the dike sections are unsafe regarding macro-stability and need improvement (see Figure 1.1 for top view of these dike sections).



Figure 1.1. IJssel-dike Krimpenerwaard Krimpen – Gouda (yellow – HM markings dike crest; red is the scope KIJK October 2015; (5) red stars indicate the location of the cross-sections (cases) in this research)

The effort and aim of POVM is wider than the project KIJK only. Intention is that methods that are developed within the cases in KIJK can be applied to other projects in The Netherlands.

The research on reliability up dating requires the following data : historical data, water levels, pore water pressures in and around the dike, subsoil layering and soil parameters etc.

These data will be used in slope stability analyses (Macro-Stability), in which the survived historical event is simulated. In case safety suffices, this analysis might be of benefit in reducing the uncertainty in the parameters and schematization that are input to the current calculations, as part of safety assessment that indicate that the dike is unsafe.

In probabilistic analysis, part of the events has an unfavourable combination of parameters that give a stability factor below 1, i.e. the strength is smaller than the load.

On the basis of a probabilistic analysis of the behaviour under a survived historical load, part of these unfavourable parameter combinations can be excluded. This gives an adjusted probability distribution of failure under design conditions. Part of the lower safety factors will be less probable, so the dike is considered to be safer.

In case of the IJssel-dike the macro-stability of the inner slope has a relatively small dependence of the river water level. Therefore, the technique of 'updated reliability' is promising for this dike.

The core of the dike consists mainly of impermeable clay in which the phreatic level is hardly influenced by the river level. The water head (pore pressure) in the sand layer beneath the dike is influenced by the water level in the river, but it was found to have little influence on slope stability, as the water head is relatively low and normative sliding circles have a limited depth.

In this framework the high water period in 1953 might have been close to the critical design circumstances, as well as historical heavy traffic loads and heavy rainfall. The closer these loads are to the design loads, the better, as more unfavourable parameter combinations might become improbable in the 'update reliability' analysis. Most favourable is a historical load that has been higher than the design circumstances.

For the purposes of the current research there are 4 dike cross-sections under consideration for which additional soil investigation is carried out.

The soil investigation consists of field investigation (cone resistance measurements, borings etc.), monitoring of the pore water pressures and laboratory investigation. This is part of activity 3 in 'POVM Beter benutten actuele sterkte'.

This report contains a review of the strength parameters from laboratory research that was executed by Wiertsema & Partners and Deltares, including the CPTu measurements. These parameters will be used in the stability analyses as described in activities 4 and 6:

- Activity 4: Using an improved calculation model (EEM) for updating macro-stability of an inner dike slope.
- Activity 6: Macro-stability will be determined by means of 'updated reliability analyses'.

## 1.2 Goal of report

This report summarises the laboratory tests conducted with in the POVM Actuele Sterkte project. The report gives an analysis of the test results and assesses the parameters needed in further in the project. Furthermore, the report provides the geotechnical background of the Actuele Sterkte project. At this point it should be noted that in detail description of the field activities performed for this project can be cited in report of Wiertsema and Partners (2016). For brevity purposes this description is omitted from this report.

## 1.3 Strategy

Dike reinforcements generally consider long dike stretches, usually tenths of kilometres. The information on loading and soil conditions needs to be relevant for the entire considered dike stretch length. As a consequence, the information on soil and loading conditions for the individual cross sections is limited. It is good engineering practice to estimate the required design parameters conservatively, such that if local information becomes available, application of this local information would lead to an equal or less conservative design. Before applying the probabilistic analysis, as discussed in the introduction, extra information for 4 cross sections along the Hollandse IJsseldijk is obtained and checked how this extra information influences the design calculations.

The extra information can be grouped as follows:

- Improvement of subsoil schematisation, Extra CPTu's and borings are conducted at the crest and toe of the cross sections. In combination with the previous conducted field work and a general geological understanding of the area the subsoil is schematised locally for each cross section. The results are presented in Appendix A. Beforehand, it was expected that due to subsoil compression and minor stability problems more anthropogenic material is available at the toe of the considered cross sections than applied in the sub soil schematisations so far.
- Laboratory tests are conducted to obtain the local strength characteristics. So far, according to the design standards, samples have been derived at different locations along the Hollandse IJsseldijk. Application of statistical methods provides safe, conservative, strength characteristics for the individual cross sections. Local information will reduce uncertainty and therefore optimise the strength characteristics.
- Deriving undrained strength characteristics, recently the WBI programme established a new working method for stability assessment. This working method is based on the critical state soil mechanics, CSSM, and is believed to provide a more realistic approach to soil strength
- Deriving subsoil parameters for Finite Element Method, FEM, applications. Part of the POVM activities is the development of a new material model, MC-SHANSEP to be used in the FEM-code PLAXIS.
- Laboratory tests are conducted to establish the influence of loading direction. Due to the active earth induce by the dike body, horizontal effective stresses are expect to differ in the direction perpendicular to the dike body and parallel to the dike. As a consequence it is hypothesised that the strength characteristics perpendicular to the dike would differ from the strength characteristics parallel to the dike. The difference is expected to be especially relevant for the soft materials like peat and clay. To test the hypothesis DSS tests are sheared both in perpendicular and parallel direction.
- In testing peat samples, size effects play a role. It is reported, Zwanenburg & Van (2015), that testing larger volumes of peat results in less conservative strength characteristics. To test these findings some large direct simple shear tests, LDSS-tests are conducted.

As mentioned above, this report summarizes the obtained extra information. In a companion report, report 1220518-005-GEO-0003, the results of stability calculations including the extra information is discussed. It should be noted that extra information was also obtained on ground water conditions. This information and consequences for the pore pressure schematisation is reported in the companion report.



## 2 Geotechnical laboratory test results

### 2.1 Laboratory testing plan

Within the framework of the POVM-AS activities a laboratory testing plan was formed which involved tests on samples retrieved from dikes along the river Hollandse IJssel. In total 47 anisotropically consolidated undrained triaxial tests (CAU), 37 direct simple shear tests (DSS) and 18 constant rate of strain oedometer tests (Ko-CRS) and 4 large direct simple shear tests (LDSS) have been performed in Wiertsema & Partners and Deltares laboratory complemented with classification tests. The samples originated from four different cross sections - herein referred to as Raai 1, 2, 4 & 5 - and from different boring locations per cross section - herein referred to as kruin or achterland.

The geological origin of the tested samples is identified based on visual observations in the laboratory and based on the geological profile as given per cross section location (refer to figures in Appendix A: Geological profile of cross sections). All tested peat samples were retrieved from the Nieuwkoop formation (referred to as 'Hollandveen'). The clay samples originated from three different layers (referred to as 'Klei met schelpen', 'Klei met plantenresten' and 'Klei\_antropogeen').

### 2.2 Static triaxial tests

Tests were conducted in accordance to CEN/ISO17892 Part 9. The clay specimens selected for triaxial compression tests were anisotropically consolidated under  $K_o = 0.45$  for the samples with a volume weight higher than  $14 \text{ kN/m}^3$  and  $K_o = 0.35$  for the samples with a volume weight less than  $14 \text{ kN/m}^3$ . These  $K_o$  - values were selected following the  $K_o$  - value recommendations provided in WBI (2017). Tests were performed both on normally consolidated samples ( $OCR=1$ ) and on samples tested at in situ stress test conditions. For the calculation of the field effective stress levels the Boussinesq's stress distribution theory was applied. Analytical information on the computation of the stress levels per boring and per sample basis is provided in Appendix B. Tests on normally consolidated samples were performed under a ratio of the applied vertical effective stress to the pre-consolidation pressure of 2.5.

The CAU test specifications per sample basis are summarized in Table 2.1 while the individual test results for each CAU test are presented in Appendix D.

Test ID	Sample Depth [NAP m]	Raai	Boring	Location	$\gamma_{wet}$ (kN/m <sup>3</sup> )	$P_c$ (kPa)	$\sigma_3'$ (kPa)	$\sigma_{vc}'$ (kPa)	Ko	Test Conditions	$t_{peak}$ (kPa)	$t_{25\%}$ (kPa)	Type of soil based on the geological profile	Lab	
M011	-0.78	1	B103	K	18.86	-	30	66	0.45	In situ	50.3	50.3	Klei met schelpen	W	
M013	-2.02	1	B103	K	18.74	-	33	74	0.45	In situ	67.9	65	Klei met schelpen	W	
M015	-2.89	1	B103	K	17.82	140	169	375.6	0.45	NC	140.2	122.8	Klei met schelpen	W	
M017	-3.78	1	B103	K	16.89	147	169	375.6	0.45	NC	136.4	110	Klei met plantenresten	W	
M019	-5.01	1	B103	K	16.21	-	40	89	0.45	In situ	54.8	44	Klei met plantenresten	W	
M023	-6.99	1	B103	K	16.15	-	47	104	0.45	In situ	74	58	Klei met plantenresten	W	
M025	-8	1	B103	K	17.9	-	51	114	0.45	In situ	73	53	Klei met plantenresten	W	
M003	-1.92	1	B104	A	17.91	-	8	18	0.45	In situ	23.5	22.5	Klei met schelpen	W	
M005	-3.03	1	B104	A	15.86	54	62	137.8	0.45	NC	58	49.7	Klei met schelpen	W	
M009	-5.09	1	B104	A	16.59	-	16	35	0.45	In situ	27.5	25	Klei met plantenresten	W	
M010	-5.38	1	B104	A	16.82	-	18	40	0.45	In situ	23	22.3	Klei met plantenresten	W	
M015	-8.07	1	B104	A	16.04	-	29	64	0.45	In situ	29.7	23	Klei met plantenresten	W	
M018	-9.65	1	B104	A	13.57	-	27	77	0.35	In situ	45.7	34.5	Klei met plantenresten	W	
M007	-0.47	2	B203	K	18.45	-	29	65	0.45	In situ	50.4	50	Klei antropogeen	W	
M011	-2.51	2	B203	K	18.36	175	203	451.1	0.45	NC	161.6	131.5	Klei met plantenresten	W	
M013	-3.62	2	B203	K	15.91	-	37	83	0.45	In situ	47.7	40.5	Klei met plantenresten	W	
M014	-3.93	2	B203	K	16.92	-	38	85	0.45	In situ	39.1	36	Klei met plantenresten	W	
M004	-2.35	2	B204	A	17.25	-	11	24	0.45	In situ	23.5	23	Klei met schelpen	W	
M005	-2.78	2	B204	A	17.34	75	90	200.0	0.45	NC	75.5	64.7	Klei met schelpen	W	
M008	-4.2	2	B204	A	16.67	-	19	42	0.45	In situ	32.7	31.3	Klei met plantenresten	W	
M010	-5.11	2	B204	A	15.6	-	23	51	0.45	In situ	40.2	36	Klei met plantenresten	W	
M017	-8.6	2	B204	A	18.1	-	39	87	0.45	In situ	57.1	50.5	Klei met plantenresten	W	
M005	0.23	4	B401	K	19.85	88	101	224.4	0.45	NC	107	105.6	Klei antropogeen	W	
M007	-0.57	4	B401	K	18.64	-	26	58	0.45	In situ	54.4	54	Klei antropogeen	W	
M008	-1.08	4	B401	K	19.17	-	28	62	0.45	In situ	44.7	44.2	Klei met schelpen	W	
M010	-2.09	4	B401	K	19.1	-	31	69	0.45	In situ	55.1	53	Klei met schelpen	W	
M013	-3.82	4	B401	K	18.76	-	36	79	0.45	In situ	53.5	50	Klei met plantenresten	W	
M014	-4.27	4	B401	K	19.1	127	141	313.3	0.45	NC	108.9	95.8	Klei met plantenresten	W	
M001	-3.5	4	B404	A	13.97	26	28	62.2	0.45	NC	23.4	19.1	Klei met plantenresten	W	
M002	-4.58	4	B404	A	13.62	-	6	16	0.35	In situ	18.6	16.7	Klei met plantenresten	W	
M004	-5.49	4	B404	A	14.32	-	10	23	0.45	In situ	20.1	18.5	Klei met plantenresten	W	
M016	-11.61	4	B404	A	15.54	-	25	56	0.45	In situ	29.2	22	Klei met plantenresten	W	
M018	-12.65	4	B404	A	16.6	-	29	65	0.45	In situ	29.3	22.5	Klei met plantenresten	W	
M013	-8.05	5	B504	A	16.09	-	28	62	0.45	In situ	26.8	19.3	Klei met plantenresten	W	
M003	-3.01	5	B504	A	13.98	-	9	23	0.35	In situ	36.9	33.5	Klei met plantenresten	W	
M002	-2.64	5	B504	A	17.24	75	70	200.0	0.35	NC	79.2	68.3	Klei met schelpen	W	
M015	-4.78	5	B503	K	17.18	-	31	69	0.45	In situ	43.8	39.5	Klei met plantenresten	W	
M009	-1.71	5	B503	K	16.75	-	27	61	0.45	In situ	64.1	Test results are considered not reliable beyond 6% of axial strain		Klei met schelpen	W
M007	-0.73	5	B503	K	18.64	101.5	118	262.2	0.45	NC	89.3	80.6	Klei met schelpen	W	
M006a	-0.13	5	B503	K	18.97	-	24	53	0.45	In situ	40.3	40	Klei antropogeen	W	
M011a	-0.83	1	B103	K	18.39	-	30	66	0.45	In situ	56.1	55.4	Klei met schelpen	D	
M003a	-1.97	1	B104	A	16.67	-	8	18	0.45	In situ	18.9	18.2	Klei met schelpen	D	
M007a	-0.53	2	B203	K	17.93	-	29	65	0.45	In situ	45.2	44.9	Klei antropogeen	D	
M008a	-4.27	2	B204	A	14.9	-	19	42	0.45	In situ	34.8	33	Klei met plantenresten	D	
M004a	-5.57	4	B404	A	14.32	-	8	23	0.35	In situ	19.1	16.4	Klei met plantenresten	D	
M006a	-0.19	5	B503	K	18	-	24	53	0.45	In situ	34.2	33.5	Klei antropogeen	D	
M009a	-1.5	5	B503	K	16.2	-	27	61	0.45	In situ	47.8	44	Klei met schelpen	D	

Where:  $\gamma_{wet}$  is wet density;  $P_c$  is the pre-consolidation pressure as derived from Ko-CRS tests where these are available;  $\sigma_3'$  is the effective confining stress;  $\sigma_{vc}'$  is the vertical effective stress at the end of consolidation;  $t_{peak}$  is the peak shear stress;  $t_{25\%}$  is the shear stress at 25% shear strain; A = Achterland; K = Kruin; W = Wiertsema & Partners and D = Deltares.

Table 2.1. Summary of the CAU tests performed

### 2.3 Direct simple shear tests

The DSS tests were conducted in accordance to Standard Test Method for Consolidated Undrained Direct Simple Shear Testing of Cohesive Soils, ASTM D 6528-07 American Society for the Testing of Materials and NORSOK standard G-0001, Annex D: Laboratory testing, Rev.2, October 2004. Tests were performed on cylindrical samples trimmed with the help of a cutting ring to dimensions of approximately 20 mm height and 63 mm internal

diameter. Lateral confinement of the samples was achieved via the use of a membrane surrounded by a stack of rigid low friction rings. Tests were performed both on normally consolidated samples ( $\text{OCR} = 1$ ) and on samples tested at in situ test conditions while samples were subjected to DSS testing under two different directions of loading; perpendicular or parallel to the dike. Samples were sheared under constant height conditions with a shearing rate of 8% per hour.

The DSS test specifications per sample basis are summarized in *Table 2.2* while the individual test results for each DSS test are presented in Appendix D.

Test ID	Sample Depth (NAP_m)	Raal	Boring	Location	$\gamma_{\text{wet}}$ (kN/m <sup>3</sup> )	$\sigma_{\text{vo}}'$ (kPa)	$P_c$ (kPa)	$\sigma_{\text{vc}}'$ (kPa)	Direction of loading	Test Conditions	$\tau_{\text{peak}}$ (kPa)	$\tau_{40\%}$ (kPa)	Type of soil based on the geological profile	Lab
M021-A	-5.76	1	B103	K	10.3	95.4	170	424.8	⊥	NC	168.5	163	Hollandveen	W
M021-B	-5.79	1	B103	K	9.77	95.4	170	424.7	//	NC	168.9	162	Hollandveen	W
M006-A	-3.38	1	B104	A	10.31	28.8	55	138	⊥	NC	54.5	53.2	Hollandveen	W
M006-B	-3.42	1	B104	A	10.1	28.8	55	138	//	NC	52.9	49.4	Hollandveen	W
M018-A	-5.89	2	B203	K	10.18	95	200	499.9	⊥	NC	191.6	187.1	Hollandveen	W
M018-B	-5.93	2	B203	K	9.92	95	200	499.9	⊥	NC	196.3	192.8	Hollandveen	W
M019-A	-6.45	2	B203	K	9.86	100	-	100	⊥	In situ	74.5	66.1	Hollandveen	W
M019-B	-6.49	2	B203	K	10.07	100	-	100	//	In situ	69.8	61.9	Hollandveen	W
M011-A	-5.61	2	B204	A	10.12	56.3	100	250	⊥	NC	95.8	90.7	Hollandveen	W
M011-B	-5.65	2	B204	A	10.16	56.3	100	250	//	NC	104.4	100.1	Hollandveen	W
M014-A	-7.33	2	B204	A	9.76	70.2	-	70	⊥	In situ	43.5	42.7	Hollandveen	W
M014-B	-7.3	2	B204	A	9.92	70.2	-	70	//	In situ	41.5	Note 1	Hollandveen	W
M007-A	-6.88	4	B404	A	9.97	32.7	55	138	⊥	NC	60.5	58.9	Hollandveen	W
M007-B	-6.92	4	B404	A	9.96	32.7	55	138	//	NC	57	56.7	Hollandveen	W
M008-A	-7.44	4	B404	A	9.92	34.9	-	35	⊥	In situ	22.7	Note 1	Hollandveen	W
M008-B	-7.47	4	B404	A	10.02	34.9	-	35	//	In situ	22.9	Note 1	Hollandveen	W
M010-A	-8.47	4	B404	A	9.75	39.9	-	40	⊥	In situ	26.8	26.1	Hollandveen	W
M010-B	-8.51	4	B404	A	9.62	39.9	-	40	//	In situ	25.2	25.5	Hollandveen	W
M010-A	-2.01	5	B503	K	11.72	62.2	-	62	⊥	In situ	61.3	57.5	Hollandveen	W
M010-B	-2.05	5	B503	K	11.35	62.2	-	61.9	//	In situ	57.4	55.4	Hollandveen	W
M017-A	-5.64	5	B503	K	9.28	77.3	145	362.8	⊥	NC	149.5	143.9	Hollandveen	W
M017-B	-5.68	5	B503	K	9.48	77.3	145	362.9	//	NC	131.3	126.9	Hollandveen	W
M004-A	-3.46	5	B504	A	11.11	29.5	55	138	⊥	NC	55.8	51.6	Hollandveen	W
M005-A	-4.08	5	B504	A	10.1	31.7	-	32	⊥	In situ	21.4	21	Hollandveen	W
M005-B	-4.04	5	B504	A	10.15	31.7	-	32	//	In situ	21.7	21.9	Hollandveen	W
M006-A	-4.47	5	B504	A	10.01	33.3	-	33	⊥	In situ	21.4	21.3	Hollandveen	W
M006-B	-4.5	5	B504	A	9.91	33	-	33	//	In situ	20.2	19.9	Hollandveen	W
M009-A	-6.08	5	B504	A	9.98	43.2	-	43	⊥	In situ	25.3	25.5	Hollandveen	W
M009-B	-6.12	5	B504	A	9.99	43.2	-	43	//	In situ	23.7	23.3	Hollandveen	W
M018b	-6.03	2	B203	K	10.79	95	-	94.5	⊥	In situ	79.5	Note 2	Hollandveen	D
M010a	-2.15	2	B203	K	12.75	74.2	-	62	⊥	In situ	57.2	56.9	Hollandveen	D
M020a	-7.02	2	B203	K	9.81	103.3	-	103	⊥	In situ	73.1	71.8	Hollandveen	D
M012b	-3.18	5	B503	K	13.73	65	-	65	⊥	In situ	54.9	54.8	Hollandveen	D
M004b	-3.6	5	B504	A	9.81	29.5	-	30	⊥	In situ	18.1	17.4	Hollandveen	D
M017b	-5.69	5	B503	K	9.81	77.3	-	77	⊥	In situ	59	57.9	Hollandveen	D
M004c	-3.55	5	B504	A	10.79	29.5	-	30	//	In situ	23.1	22.9	Hollandveen	D
M021b	-5.93	1	B103	K	11.77	95.4	-	94.7	//	In situ	70.3	64.1	Hollandveen	D

Where:  $\gamma_{\text{wet}}$  is wet density;  $\sigma_{\text{vo}}'$  is the in situ effective stress;  $P_c$  is the pre-consolidation pressure as derived from Ko-CRS tests where these are available;  $\sigma_{\text{vc}}'$  is the vertical effective stress at the end of consolidation;  $\tau_{\text{peak}}$  is the peak shear stress;  $\tau_{40\%}$  is the shear stress at 40% shear strain; A = Achterland; K = Kruin; W = Wiertsema & Partners; D = Deltares; ⊥ = perpendicular and // = parallel.

Note 1: Test results are considered not reliable beyond 20% of shear strain.

Note 2: Data available only up to 19% of shear strain.

Table 2.2. Summary of the DSS tests performed

## 2.4 Ko-CRS tests

The CRS tests were conducted in accordance to Standard Test Method for One-Dimensional Consolidation Properties of Soils Using Controlled-Strain Loading, ASTM D 4186 – 06 American Society for the Testing of Materials. Deltares has developed a CRS device that also measures the horizontal stresses, Den Haan & Kamao (2003). In total 18 Ko-CRS tests were conducted.

The Ko-CRS test specifications per sample basis are summarized in *Table 2.3* while the individual test results for each Ko-CRS test are presented in Appendix E.

Test ID	Sample Depth [NAP_m]	Raai	Boring	Location	$\gamma_{wet}$ (kN/m <sup>3</sup> )	Type of soil based on the geological profile	Laboratory
M017a	-4.02	1	B103	Kruin	14.6	Klei met plantenresten	Deltares
M021a	-5.96	1	B103	Kruin	9.8	Hollandveen	Deltares
M006a	-3.62	1	B104	Achterland	9.4	Hollandveen	Deltares
M005a	-2.85	2	B204	Achterland	16.0	Klei met plantenresten	Deltares
M011a	-5.82	2	B204	Achterland	9.3	Hollandveen	Deltares
M014a	-4.36	4	B401	Kruin	19.4	Klei met plantenresten	Deltares
M001a	-3.55	4	B404	Achterland	13.5	Klei met plantenresten	Deltares
M007a	-7.07	4	B404	Achterland	9.5	Hollandveen	Deltares
M007a	-0.82	5	B503	Kruin	19.9	Klei met schelpen	Deltares
M012a	-3.24	5	B503	Kruin	12.6	Based on visual observations the soil is classified as clay. Based on the geological profile the soil is classified as peat.	Deltares
M005a	0.14	4	B401	Kruin	21.7	Klei_antropogeen	Deltares
M002a	-2.72	5	B504	Achterland	15.5	Klei met plantenresten	Deltares
M017a	-5.76	5	B503	Kruin	10.4	Hollandveen	Deltares
M004a	-3.66	5	B504	Achterland	9.6	Hollandveen	Deltares
M018c	-5.96	2	B203	Kruin	10.7	Hollandveen	Deltares
M004b	-2.46	1	B104	Achterland	15.4	Klei met schelpen	Deltares
M015b	-2.96	1	B103	Kruin	16.5	Klei met schelpen	Deltares
M011b	-2.59	2	B203	Kruin	14.9	klei met plantenresten	Deltares

*Table 2.3 Summary of the Ko-CRS tests performed*

## 2.5 Large DSS tests, LDSS

A total of 4 LDSS tests were performed at in situ stress conditions. As was the case for the DSS so for the LDSS tests the samples were subjected to two different directions of loading; perpendicular or parallel to the dike.

Rectangular samples with a length (parallel to the shearing direction) of 260 mm, a width of 220 mm and a height after consolidation of approximately 80 mm were tested.

Tests were performed following as closely as possible the conventional DSS testing procedures (Standard Test Method for Consolidated Undrained Direct Simple Shear Testing of Cohesive Soils, ASTM D 6528-07 American Society for the Testing of Materials and

NORSOK standard G-0001, Annex D: Laboratory testing, Rev.2, October 2004) while for the parts of the testing procedure which differentiates from the conventional DSS tests, the Deltares LDSS In-House procedures were applied. Further details of the LDSS equipment are given by Den Haan & Grognet (2014).

The LDSS test specifications per sample basis are summarized in *Table 2.4* while the individual test results for each LDSS test are presented in Appendix F.

Samples were sheared under constant height conditions with a shearing rate of 8% per hour while testing was terminated up on reaching a maximum shear strain of 40%.

a/a	Test ID	Sample Depth (NAP_m)	Raai	Boring	Location	$\sigma_{vc}'$ (kPa)	Direction of loading	Test Conditions	$\tau_{peak}$ (kPa)	$\tau_{40\%}$ (kPa)
1	DLDS-B1	-3.35	5	DLDS-B	Toe of the dike	23.5	⊥	In situ	22.5	22
2	DLDS-B2	-3.24	5	DLDS-B	Toe of the dike	23.5	//	In situ	22.2	22
3	DLDS-A3	-4.27	5	DLDS-A	Toe of the dike	23.5	⊥	In situ	20.3	20
4	DLDS-A4	-4.15	5	DLDS-A	Toe of the dike	23.5	//	In situ	14.4	14.4

Where  $\sigma_{vc}'$  is the vertical effective stress at the end of consolidation;  $\tau_{peak}$  is the peak shear stress;  $\tau_{40\%}$  is the shear stress at 40% shear strain; ⊥ =perpendicular and // =parallel to the dike.

*Table 2.4 Summary of the LDSS tests performed*

## 2.6 Index laboratory tests

Table 2.5 lists the index classification tests performed and the standards/procedures as followed per type of test.

Type of test	Test Procedure/Standard
Atterberg limits	Plastic limit is determined as the moisture content for which 3 mm soil thread can be rolled by hand. For the determination of the Liquid limit the Casagrande method was used. For further details on the testing procedure refer to report of Wiertsema and Partners (2016).
Particle size distribution	The Particle Size Distribution (PSD) was assessed via the use of sieves for the part of soil with particles >63 microns while for smaller sizes the particle distribution was assessed via the use of Stokes' law. For further details on the testing procedure refer to the report of Wiertsema and Partners (2016).
Organic matter	Depending on the type of soil two different methods were used; (a) LOI and (b) oxidization with H <sub>2</sub> O <sub>2</sub> . For further details on the testing procedure refer to the report of Wiertsema and Partners (2016).
Calcium content	Depending on the type of soil two different methods were used; (a) LOI and (b) Addition of HCL. For further details on the testing procedure refer to the report of Wiertsema and Partners (2016).

*Table 2.5 Testing procedures/standards per type of test performed*



- A total of 21 Atterberg limits tests were performed. The test results of these tests are presented in Appendix G.
- A total of 21 Particle Size Distribution (PSD) tests were performed. The test results for these tests are presented in Appendix H.
- A total of 21 organic matter content and 21 calcium content tests were performed. The test results from these tests are summarized in the test report presented in Appendix I.

### 3 Soil parameter assessment

#### 3.1 Geotechnical laboratory test results

##### 3.1.1 General

This section of the report includes the analysis of the laboratory tests results with the main objective to obtain the required geotechnical parameters that will be used as input in the FEM and LEM calculations. The analysis of the data focusses in the assessment of the undrained and drained shear strength parameters and stiffness characteristics. The derived parameters are discussed while average and characteristic values are provided when these are available. The quality of the laboratory test results is evaluated while any up normalities in the testing procedure/test results are reported.

##### 3.1.2 Assessment of undrained shear strength

The undrained shear strength values as derived from each tested sample are summarized in in *Table 2.1* and *Table 2.2* for the case of the CAU and DSS tests respectively. Values of the undrained peak shear strength and undrained shear strength at large strains (25% axial strain for the CAU tests and 40% shear strain for the DSS tests) are shown.

In regards to the quality assessment of the data it should be mentioned that:

- The CAU stress path of sample M009 (Raai 5, Boring 503) exhibited an up normal trend behaviour after the formation of a peak shear strength. Thus, for this sample, the test result data beyond the peak shear strength and for axial strain in excess of 6% are not considered reliable and are omitted from *Table 2.1*.
- The DSS test result data of samples M014-B (Raai 2, Boring 203), M008-A (Raai 4, Boring 404) and M008-B (Raai 4, Boring 404) are not considered reliable beyond a shear strain of 20%. The relevant data are therefore omitted from *Table 2.2*.
- For sample M018b (Raai 2, Boring 203) the DSS test result data are available only up to approximately 19% of shear strain.

Due to the presence of the dike the ground beneath the toe of the dike might have been subjected to simple shear pre-shearing in the direction perpendicular to the dike resulting in the occurrence of an initial static shear stress. The loading direction of the samples in reference to their pre-shearing direction could have an influence on the undrained shear behaviour of the samples examined in the laboratory. To assess experimentally whether this hypothesis can be valid the DSS tests in this project were performed under two different directions of loading. That is:

- (a) Perpendicular to the dike (22 tests)
- (b) Parallel to the dike (15 tests)

The undrained shear strength values at peak and at 40% shear strain are plotted versus the effective vertical stress at the end of consolidation in *Figure 3.1* and *Figure 3.2* respectively.

The test data corresponding to the samples sheared perpendicular to the dike are indicated with green circle marks while the test data of the samples sheared parallel to the dike are

indicated with red triangle marks. The above figures include data for tests performed both under in situ and normally consolidated conditions.

It can be observed that there is no apparent influence of the direction of loading on the undrained shear strength values - both at peak and at 40% shear strain - with the test data at different loading directions practically coinciding for the same vertical effective stress level.

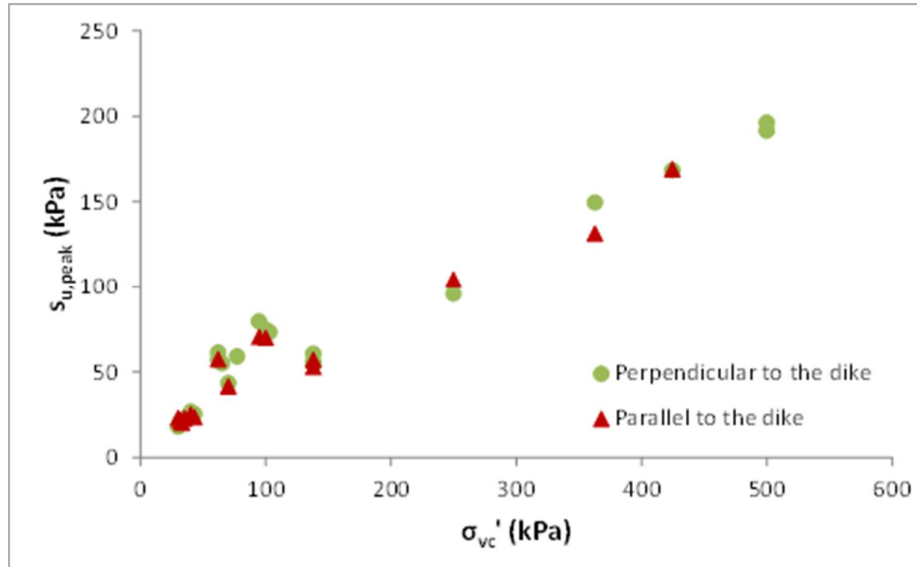


Figure 3.1 DSS test results; effect of direction of loading on the undrained shear strength at peak

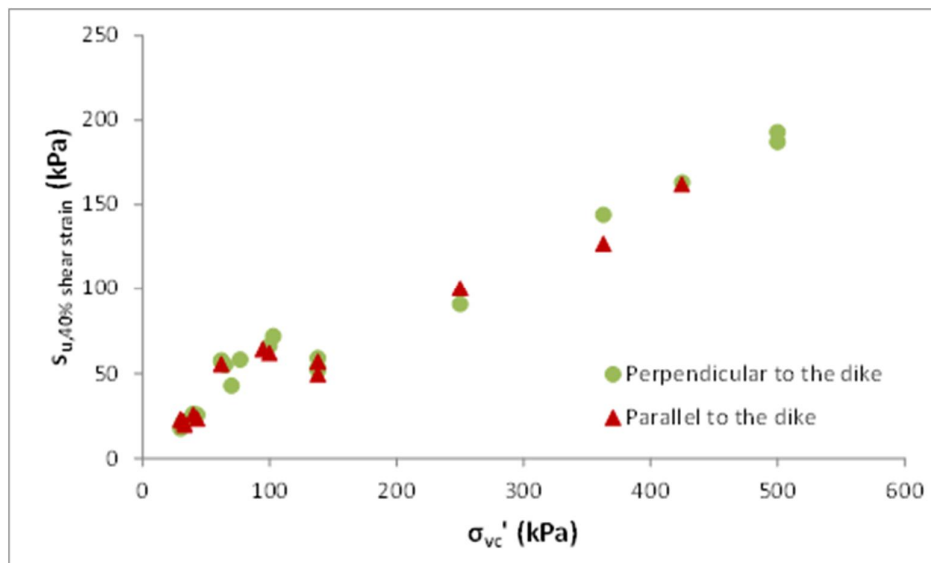


Figure 3.2 DSS test results; effect of direction of loading on the undrained shear strength at 40% shear strain



### 3.1.3 Assessment of shear strength ratio

For the samples tested under normally consolidated conditions ( $OCR = 1$ ), the undrained shear strength ratio  $S$  has been calculated at 25% axial strain for the case of CAU tests and at 40% shear strain for the case of DSS tests. For normally consolidated conditions the undrained shear strength ratio,  $S$ , is defined as:

$$S = \left( \frac{s_u}{\sigma'_{vc}} \right)_{NC} \quad (1)$$

Where:

- $s_u$  = the soil's undrained shear strength and
- $\sigma'_{vc}$  = the vertical effective stress at the end of consolidation.

The test specifications of the normally consolidated samples are summarized in *Table 3.1* for the case of CAU tests and in *Table 3.2* for the case of the DSS tests.

An overview of the calculated  $S$  ratio values for the tested clay and peat samples is given in *Figure 3.3* and *Figure 3.4* respectively. In these figures the  $S$  ratio values are plotted against the sample's volumetric weight. For comparison purposes a distinction of the data per sampling location (kruin or achterland) and per material type (Klei met schelpen; klei met plantenresten and Klei antropogeen for the case of clay samples) is also provided in these figures.

For the analysis of the data to follow the average, standard deviation and characteristic values are calculated according to the equations:

$$x_{gem} = \frac{\sum_{i=1}^{x=n} (x_i \dots x_n)}{n} \quad (2)$$

$$\sigma_x = \sqrt{\frac{\sum_{i=1}^{x=n} (x_i - x_{gem})^2}{n-1}} \quad (3)$$

$$x_{kar} = x_{gem} - \sigma_x \times t_{0,1;n-1} \times \sqrt{\frac{1}{n} + (1-\alpha)} \quad (4)$$

Where:

- $x_{gem}$  = the average value of parameter  $x$ ;
- $x_{kar}$  = the characteristic 5% lower limit value of parameter  $x$ ;
- $n$  = number of tests;
- $\sigma_x$  = is the standard variation of parameter  $x$ ;
- $t_{0,1;n-1}$  = the 10% value of the Student-t distribution and
- $\alpha$  = the data distribution parameter.

For the calculation of the characteristic  $S$  value a regional data distribution parameter of  $\alpha = 0.75$  is considered since the data used in the calculations are derived from different cross sections and boring locations of the investigated area.

To evaluate whether the differences in the calculated S ratio values from different clay layers are statistically significant the Wilcoxon Rank Sum test is applied to the data. This evaluation is limited in a single pair of clay layers (klei met schelpen and klei met plantenresten) since for the case of klei antropogeen only one S ratio measurement is available.

Based on the outcome of the above test, for a level of significance of 0.05 ( $\alpha = 0.05$ ) and for both a two tailed and one tailed test the difference among the S ratio values from 'klei met schelpen' and 'klei met plantenresten' is deemed to be significant.

Since the number of tests performed per clay layer is rather limited it is decided, contrary to the outcome of the Wilcoxon Rank Sum test, to assess a unique S ratio value for all the data regardless of the origin of the samples. The larger group of data provide a less conservative S ratio value. As can be seen in *Figure 3.3*, which includes all the data available, the difference in the actual S ratio values among samples from different clay layers is relatively small.

For the CAU tests, and for a normal distribution of the data, the calculated average value of the shear strength ratio,  $\mu$ , the standard deviation,  $\sigma$ , and the characteristic value,  $S_{kar}$ , are as follows:

- $\mu = 0.317, \sigma = 0.023$
- $S_{kar} = 0.29$

As discussed above these values have been derived based on the set of the CAU test data presented in *Table 3.1* regardless of the sampling location and the origin of the samples. It should be noted though that the S ratio value of the Sample M005 – B401 ( $S=0.47$ ) is discarded from the analysis of data since this value is considered unjustifiably too high.

For the DSS tests, and for a normal distribution of the data:

- $\mu = 0.384, \sigma = 0.021$
- $S_{kar} = 0.36$

These values have been derived based on the set of the DSS test data presented in *Table 3.2* without any distinction of the data per sampling location and per loading direction (parallel or perpendicular to the dike). As can be seen in *Figure 3.2* and *Figure 3.4* there is no apparent influence of these factors on the calculated S ratio values.

a/a	Test ID	Raai	Boring	Loca- tion	$v_{wet}$ (kN/m <sup>3</sup> )	$\sigma_{vc}'$ (kPa)	$t_{peak}$ (kPa)	$t_{25\%}$ (kPa)	$(s_u/\sigma_{vc}')_{25\%}$ axial strain	Testing Conditions	Type of soil based on the geological profile
1	M015	1	B103	K	17.8	375.6	140.2	122.8	0.33	NC	Klei met schelpen
2	M017	1	B103	K	16.9	375.6	136.4	110	0.29	NC	Klei met plantenresten
3	M005	1	B104	A	15.9	137.8	58	49.7	0.36	NC	Klei met schelpen
4	M011	2	B203	K	18.4	451.1	161.6	131.5	0.29	NC	Klei met plantenresten
5	M005	2	B204	A	17.3	200.0	75.5	64.7	0.32	NC	Klei met schelpen
6	M005	4	B401	K	19.8	224.4	107	105.6	0.47	NC	Klei_antropogeen
7	M014	4	B401	K	19.1	313.3	108.9	95.8	0.31	NC	Klei met plantenresten
8	M001	4	B404	A	14.0	62.2	23.4	19.1	0.31	NC	Klei met plantenresten
9	M002	5	B504	A	17.2	200.0	79.2	68.3	0.34	NC	Klei met schelpen
10	M007	5	B503	K	18.6	262.2	89.3	80.6	0.31	NC	Klei met schelpen

Table 3.1 Summary of the normally consolidated CAU tests performed\_Peak shear stress, shear stress at 25% axial strain and S ratio values

a/a	Test ID	Raai	Boring	Loca- tion	$v_{wet}$ (kN/m <sup>3</sup> )	$\sigma_{vc}'$ (kPa)	$\tau_{peak}$ (kPa)	$\tau_{40\%}$ (kPa)	$(s_u/\sigma_{vc}')_{40\%}$ shear strain	Direction of loading	Testing Conditions	Type of soil based on the geological profile
1	M021-A	1	B103	K	10.3	424.8	168.5	163	0.38	⊥	NC	Hollandveen
2	M021-B	1	B103	K	9.8	424.7	168.9	162	0.38	//	NC	Hollandveen
3	M006-A	1	B104	A	10.3	138	54.5	53.2	0.39	⊥	NC	Hollandveen
4	M006-B	1	B104	A	10.1	138	52.9	49.4	0.36	//	NC	Hollandveen
5	M018-A	2	B203	K	10.2	499.9	191.6	187.1	0.37	⊥	NC	Hollandveen
6	M018-B	2	B203	K	9.9	499.9	196.3	192.8	0.39	⊥	NC	Hollandveen
7	M011-A	2	B204	A	10.1	250	95.8	90.7	0.36	⊥	NC	Hollandveen
8	M011-B	2	B204	A	10.2	250	104.4	100.1	0.40	//	NC	Hollandveen
9	M007-A	4	B404	A	10.0	138	60.5	58.9	0.43	⊥	NC	Hollandveen
10	M007-B	4	B404	A	10.0	138	57	56.7	0.41	//	NC	Hollandveen
11	M017-A	5	B503	K	9.3	362.8	149.5	143.9	0.40	⊥	NC	Hollandveen
12	M017-B	5	B503	K	9.5	362.9	131.3	126.9	0.35	//	NC	Hollandveen
13	M004-A	5	B504	A	11.1	138	55.8	51.6	0.37	⊥	NC	Hollandveen

Table 3.2 Summary of the normally consolidated DSS tests performed\_Peak shear stress, shear stress at 40% shear strain and S ratio values

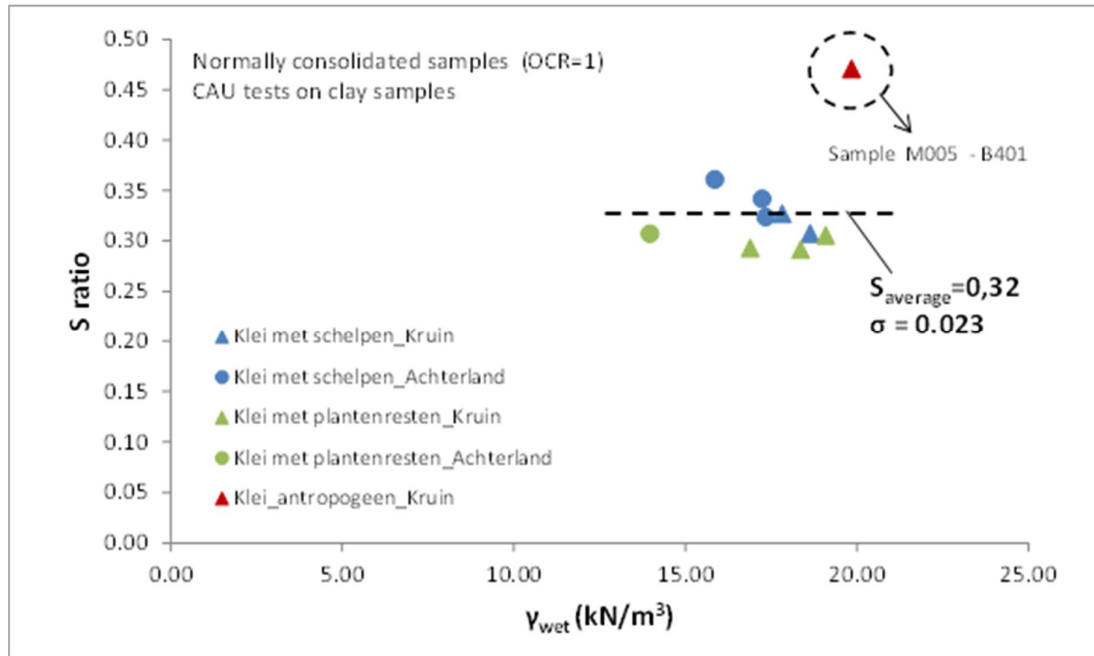


Figure 3.3. S ratio versus volumetric weight; clay samples

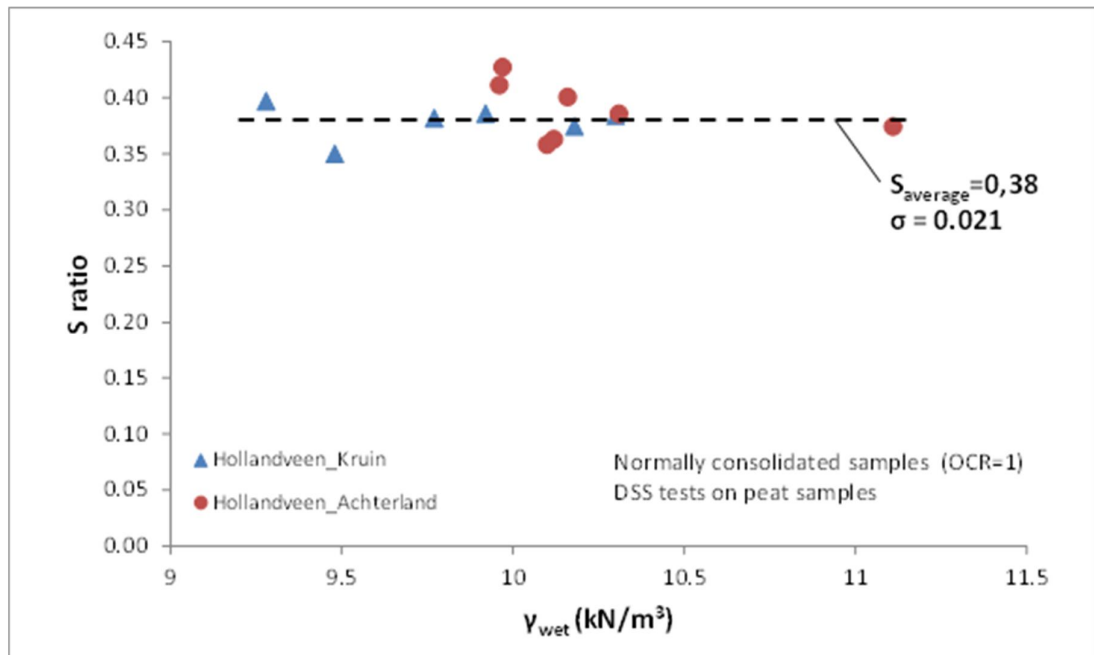


Figure 3.4. S ratio versus volumetric weight; peat samples.

To avoid the presence of negative values in probabilistic calculations the lognormal distribution of data is used. For the CAU data the use of a lognormal distribution results in an average value of the shear strength ratio of  $\mu_{(log)}$  with a standard deviation  $\sigma_{(log)}$  (where  $\mu_{(log)}$

stands for mean and  $\sigma_{(\log)}$  for standard deviation of the correspondent probability density function - PDF) as follow:

- $\mu_{(\log)} = 0.317$
- $\sigma_{(\log)} = 0.014$

A lognormal distribution of the DSS data, results in:

- $\mu_{(\log)} = 0.383$
- $\sigma_{(\log)} = 0.013$

The above lognormal distribution parameters have been derived on the same set of data used for calculating the relevant normal distribution parameters. It can be observed for both the CAU and DSS sets of data that the use of lognormal distribution fits slightly better the experimental data since lower standard deviation values are obtained.

Table 3.3 provides an overview of the characteristic, mean and standard deviation values as assessed per type of soil in this study.

Type of soil	S <sub>kar</sub>	Normal distribution		Lognormal distribution	
		$\mu$	$\sigma$	$\mu_{(\log)}$	$\sigma_{(\log)}$
Clay	0.29	0.317	0.023	0.317	0.014
Peat	0.36	0.384	0.021	0.383	0.013

Table 3.3 Summary of characteristic, mean and standard deviation values per type of soil

To account for the fluctuation of soil properties in the vertical dimension relative to the direction of the slip plane, local averaging along the slip plane needs to be implemented in the slope stability analysis calculations. Local averaging and uncertainty for the number of samples are accounted in the calculations of the standard deviation according to the equation by Van Deen and Van Duinen (2016):

$$\sigma_{loc,aver} = \sigma_{reg} \sqrt{(1-\alpha) + 1/n} \quad (5)$$

Where:

- $\sigma_{loc,aver}$  = the local, average standard deviation ;
- $\sigma_{reg}$  = the standard deviation of the regional variation;
- $\alpha$  = the portion of the total variability stemming from local variability (for regional sampling  $\alpha = 0.75$ ) and
- $n$  = the number of the regional samples.

### 3.1.4 Assessment of stiffness parameters

In FEM computations the use of advanced materials models such as the Soft Soil (SS) and Shansep MC model require as input, information on the soil's compression, swelling and stress history indices. In summary the following parameters need to be determined:

- Modified compression,  $\lambda^*$ , swelling,  $\kappa^*$ , and creep,  $\mu^*$  indices;
- Poisson's ratio,  $\nu_{ur}$ , for unloading/reloading;
- $K_o^{NC}$  coefficient of lateral stress in normal consolidation and

- Over-Consolidation Ratio, OCR.

The above parameters were obtained in this study from Ko-CRS tests as follows:

- The parameters  $\kappa^*$ ,  $\lambda^*$  were calculated from plots of the logarithm of the mean effective stress,  $p'$ , as a function of the volumetric strain, the slope of the primary loading line gives the value of the modified compression index  $\lambda^*$  and the slope of the unloading line gives the modified index  $\kappa^*$ . The  $\mu^*$  parameter was calculated from the relaxation phase of the test by fitting of mean effective stress  $p'$  and time data to the laboratory test results. Where  $p' = \frac{\sigma'_v + 2\sigma'_h}{3}$ , with  $\sigma'_v$  and  $\sigma'_h$  being the vertical and horizontal effective stress respectively.
- The parameter  $m$  was calculated according to the equation:

$$m = \frac{b - a}{b} \quad (6)$$

Where:  $a$  and  $b$  are the stiffness parameters of the abc - isotachen model.

- The isotachen model parameters  $a$ ,  $b$  and  $c$  were calculated from plots of the logarithm of the effective vertical stress,  $\sigma'_v$ , as a function of the natural strain,  $\epsilon^H$  (the slope of the primary loading line gives the value of the modified compression index,  $b$ , and the slope of the unloading lines gives the modified index  $a$ ). The  $c$  parameter was calculated from the relaxation phase of the test by fitting the effective vertical stress,  $\sigma'_v$ , and time data to the laboratory test results.
- The Poisson's ratio,  $\nu_{ur}$  was calculated at the unloading – reloading phase of the test.
- The values of OCR were calculated based on the values of pre-consolidation pressure estimated in accordance with the NEN procedure method. OCR is defined as the ratio of pre-consolidation pressure to the vertical in situ effective stress.

The values of  $Ko^{NC}$ ; OCR; preconsolidation pressure; Poisson's ratio,  $\nu_{ur}$ ; isotachen model stiffness parameters  $a$ ,  $b$ ,  $c$ ;  $m$ ; the modified cam clay model parameters,  $\kappa^*$ ;  $\lambda^*$  and  $\mu^*$  as these were derived from the Ko-CRS data are shown in Table 3.4 and Table 3.5 for the case of clay and peat samples respectively.

Test ID	Sample Depth [NAP_m]	Raai	Boring	Location	$\gamma_{wet}$ (kN/m <sup>3</sup> )	$P_{c\_NEN}$ (kPa)	$P_{c\_Isot.}$ (kPa)	$\sigma_{vo}'$ (kPa)	OCR	POP	$v_{ur}$	$\alpha$	b	c	$\kappa^*$	$\lambda^*$	$\mu^*$	Ko	m	Type of soil based on the geological profile					
M017a	-4.02	1	B103	K	14.6	142.4	146.7	84.7	1.7	57.7	0.240	0.012	0.119	0.006	0.012	0.099	0.004	0.45	0.899	Klei met plantenresten					
M005a	-2.85	2	B204	A	16.0	72.1	75.5	29.0	2.5	43.1	0.190	0.052	0.078	0.004	0.005	0.062	0.003	0.48	0.333	Klei met plantenresten					
M014a	-4.36	4	B401	K	19.4	123.8	126.8	82.8	1.5	41.0	0.260	0.005	0.053	0.002	0.006	0.047	0.002	0.46	0.898	Klei met plantenresten					
M001a	-3.55	4	B404	A	13.5	20.4	25.8	9.6	2.1	10.8	0.230	0.013	0.197	0.011	0.013	0.142	0.008	0.48	0.934	Klei met plantenresten					
M007a	-0.82	5	B503	K	19.9	97.7	101.5	56.4	1.7	41.3	0.260	0.004	0.055	0.002	0.004	0.047	0.002	0.46	0.927	Klei met schelpen					
M012a	-3.24	5	B503	K	12.6	116.9	123.1	64.6	1.8	52.3	0.200	0.015	0.131	0.009	0.013	0.098	0.005	0.35	0.885	Based on visual observations the soil is classified as clay. Based on the geological profile the soil is classified as peat.					
M005a	0.14	4	B401	K	21.7	85.3	88.2	51.0	1.7	34.3	0.250	0.006	0.055	0.002	0.008	0.051	0.001	0.48	0.891	Klei antropogeen					
M002a	-2.72	5	B504	A	15.5	72.2	75.3	21.9	3.3	50.3	0.120	0.004	0.067	0.004	0.003	0.051	0.003	0.31	0.945	Klei met plantenresten					
M004b	-2.46	1	B104	A	15.4	52.0	56.3	22.3	2.3	29.7	0.220	0.007	0.107	0.005	0.004	0.084	0.005	0.41	0.935	Klei met schelpen					
M015b	-2.96	1	B103	K	16.5	137.2	140.4	79.7	1.7	57.5	0.230	0.007	0.089	0.005	0.007	0.073	0.003	0.42	0.921	Klei met schelpen					
M011b	-2.59	2	B203	K	14.9	169.2	174.9	76.9	2.2	92.3	0.170	0.011	0.124	0.007	0.010	0.096	0.004	0.32	0.911	Klei met plantenresten					
															Average:	0.008	0.077	0.003	0.43	0.918					
															Standard Deviation:	0.0036	0.0300	0.0018	0.0324	0.021					

Table 3.4 Summary of soil parameters as derived from Ko-CRS tests for clay samples

Test ID	Sample Depth [NAP_m]	Raai	Boring	Location	$\gamma_{wet}$ (kN/m <sup>3</sup> )	$P_{c\_NEN}$ (kPa)	$P_{c\_Isot.}$ (kPa)	$\sigma_{vo}'$ (kPa)	OCR	POP	$v_{ur}$	$\alpha$	b	c	$\kappa^*$	$\lambda^*$	$\mu^*$	Ko	m						
M021a	-5.96	1	B103	K	9.8	162.5	170.300	95.4	1.703	67.1	0.170	0.036	0.316	0.022	0.031	0.218	0.010	0.270	0.886						
M006a	-3.62	1	B104	A	9.4	45.8	53.500	29.0	1.579	16.8	0.100	0.033	0.336	0.024	0.041	0.231	0.013	0.300	0.902						
M011a	-5.82	2	B204	A	9.3	86.1	100.600	56.3	1.529	29.8	0.180	0.041	0.293	0.022	0.028	0.185	0.009	0.270	0.860						
M007a	-7.07	4	B404	A	9.5	42.9	55.100	32.7	1.312	10.2	0.220	0.042	0.301	0.021	0.037	0.222	0.009	0.310	0.860						
M017a	-5.76	5	B503	K	10.4	119.8	142.200	77.3	1.550	42.5	0.160	0.039	0.322	0.030	0.031	0.212	0.013	0.240	0.879						
M004a	-3.66	5	B504	A	9.6	41.0	53.100	29.5	1.390	11.5	0.230	0.031	0.262	0.020	0.024	0.171	0.010	0.290	0.882						
M018c	-5.96	2	B203	K	10.7	179.6	190.700	95.0	1.891	84.6	0.190	0.028	0.280	0.019	0.021	0.198	0.010	0.220	0.900						
															Average:	0.030	0.205	0.010	0.27	0.881					
															Standard Deviation:	0.0070	0.0216	0.0019	0.0324	0.017					

Where  $\gamma_{wet}$  is the volumetric weight;  $P_c$  is the pre-consolidation pressure and  $\sigma_{vo}'$  is the in-situ stress.

Table 3.5 Summary of soil parameters as derived from Ko-CRS tests for peat samples

Based on the available data the average and standard deviation of the calculated  $\kappa^*$ ,  $\lambda^*$ ,  $\mu^*$  values are as follows:

For the clay samples

$$\begin{aligned} \kappa^*_{average} &= 0.008 \text{ with } \sigma = 0.0036 \\ \lambda^*_{average} &= 0.077 \text{ with } \sigma = 0.0300 \\ \mu^*_{average} &= 0.003 \text{ with } \sigma = 0.0018 \end{aligned}$$

For the peat samples

$$\begin{aligned} \kappa^*_{average} &= 0.030 \text{ with } \sigma = 0.0070 \\ \lambda^*_{average} &= 0.205 \text{ with } \sigma = 0.0216 \\ \mu^*_{average} &= 0.010 \text{ with } \sigma = 0.0019 \end{aligned}$$

The average and standard deviation of the calculated  $K_o$  values are as follows:

For the clay samples

$$K_o^{NC} = 0.43 \text{ with } \sigma = 0.0638$$

For the peat samples

$$K_o^{NC} = 0.27 \text{ with } \sigma = 0.0324$$

It should be noted that the  $\kappa^*$ ,  $\lambda^*$ ,  $\mu^*$  and  $K_o^{NC}$  values do not appear to be influenced by changes of the sampling location (changes of cross section and boring location) at least for the investigated area under consideration. For the clay layers no obvious changes of the above values are noted among different types of clay (Klei met plantenresten, Klei met schelpen, Klei\_antropogeen).

*Parameter, m*

For the clay samples, and for a normal distribution of the data:

- $\mu_m = 0.918$ ,  $\sigma_m = 0.021$
- $m_{kar} = 0.893$

As can be seen in *Figure 3.5* the  $m$  values under consideration appear to be independent of the boring location (kruin of achterland) and the type of soil.

For the test M005a (Raai 2, Boring 204) an  $m$  value of 0.333 is calculated. This value is too low and outside the expected range of values for the encountered soil conditions and has thus been excluded from the analysis of the data.

The Wilcoxon Rank Sum test is used to evaluate the difference between each set of  $m$  values as calculated from the different clay layers. This evaluation is limited in a single pair of clay layers (klei met schelpen and klei met plantenresten) since for the case of klei antropogeen only one  $m$  value measurement is available.

Based on the outcome of the above test, for a significant level of 0.05 ( $\alpha=0.05$ ) and for both a two tailed and one tailed test the difference among the  $m$  values from 'klei met schelpen' and 'klei met plantenresten' are deemed to be insignificant.

For the peat samples, and for a normal distribution of the data:

- $\mu_m = 0.881$ ,  $\sigma_m = 0.017$
- $m_{kar} = 0.863$

As can be seen in *Figure 3.6* the  $m$  values under consideration appear to be independent of the boring location (kruin or achterland).

A regional data distribution parameter of  $\alpha=0.75$  is used for the determination of the characteristic value,  $m_{kar}$ .



A lognormal distribution of the data for the clay samples, results in an average value of  $m$   $\mu_{(\log, m)} = 0.918$  with  $\sigma_{(\log, m)} = 0.012$ .

A lognormal distribution of the data for the peat samples, results in an average value of  $m$   $\mu_{(\log, m)} = 0.881$  with  $\sigma_{(\log, m)} = 0.011$ .

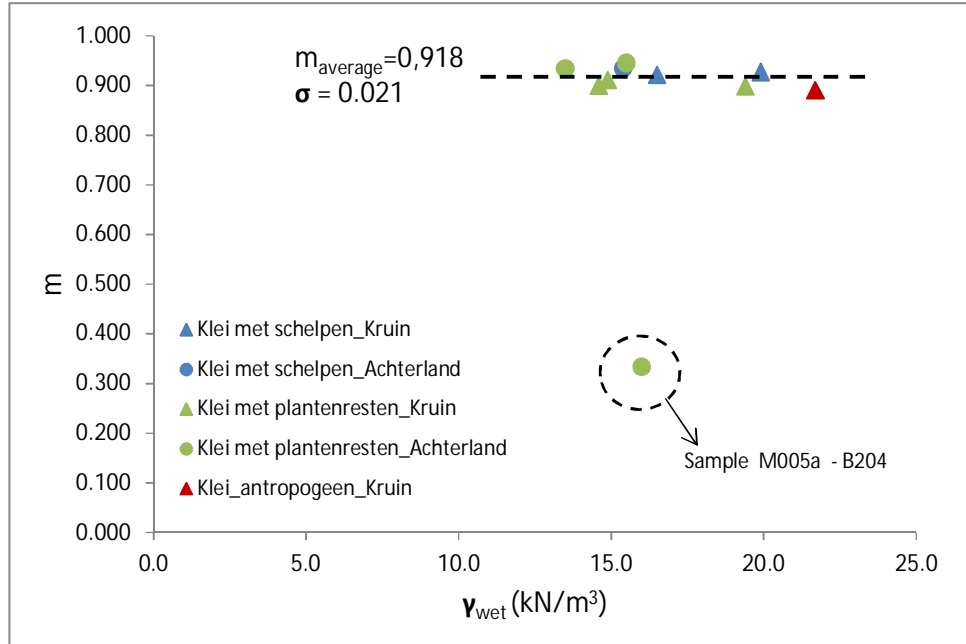


Figure 3.5  $m$  values against volumetric weight for clay samples

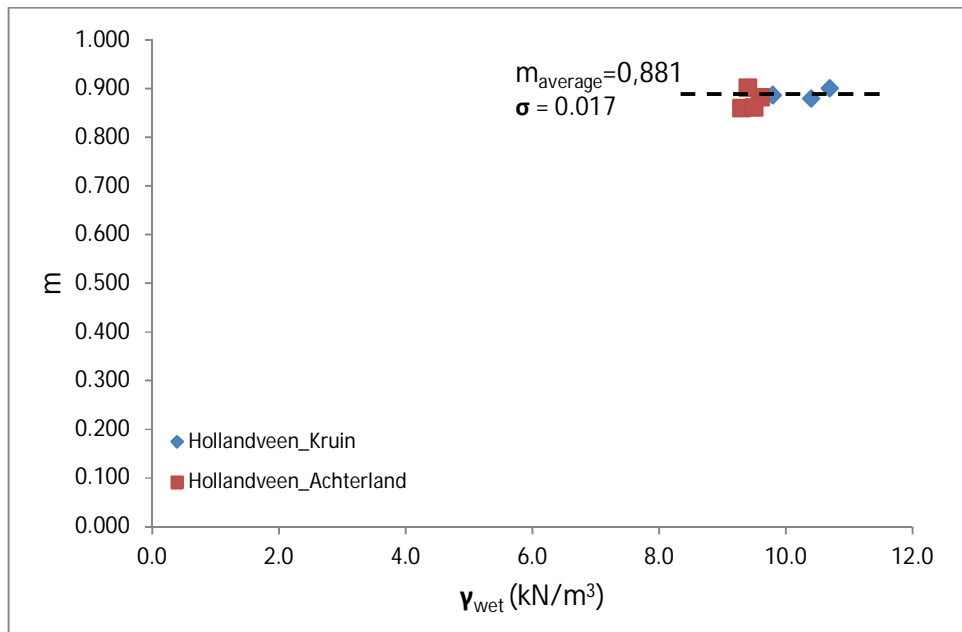


Figure 3.6:  $m$  values against volumetric weight for peat samples



The average, 5% lower/upper confidence limit and physically realizable lower limit t-s' lines can be seen in *Figure 3.8* (for 2% axial strain), *Figure 3.9* (for peak shear stress) and *Figure 3.10* (for 25% axial strain).

For the normally consolidated DSS tests the  $c'_{average}$  and  $\phi'_{average}$  and  $c'_{kar}$  and  $\phi'_{kar}$  values have been calculated at shear strain of 5% and 40% and peak shear stress. The derived values are as follows:

- $\Phi'_{average, peak}$  ,  $C'_{average, peak}$  = 28.3<sup>0</sup>, 4.40 kPa
- $\Phi'_{average, 40\% \text{ shear strain}}$  ,  $C'_{average, 40\% \text{ shear strain}}$  = 29.3<sup>0</sup>, 7.48 kPa
- $\Phi'_{average, 5\% \text{ shear strain}}$  ,  $C'_{average, 5\% \text{ shear strain}}$  = 14.8<sup>0</sup>, 9.05 kPa
- $\Phi'_{kar, peak}^{*1}$  ,  $C'_{kar, peak}$  = 26.6<sup>0</sup>, 0 kPa
- $\Phi'_{kar, 40\% \text{ shear strain}}$  ,  $C'_{kar, 40\% \text{ shear strain}}$  = 28.4<sup>0</sup>, 0.41 kPa
- $\Phi'_{kar, 5\% \text{ shear strain}}$  ,  $C'_{kar, 5\% \text{ shear strain}}$  = 14<sup>0</sup>, 0.02 kPa

\*1  $c'_{kar}$  was taken equal to zero while the  $\phi'_{kar}$  value was adjusted to produce data that fit as closely as possible the 5% lower confidence limit line.

The average, 5% lower/upper confidence limit and physically realizable lower limit t-s' lines can be seen in *Figure 3.11* (for 5% shear strain), *Figure 3.12* (for peak shear stress) and *Figure 3.13* (for 40% shear strain).

The drained shear strength parameters have been assessed at the axial strain level of 2% and shear strain level of 5 % in order to be consistent to the geotechnical approach for effective stress analysis reported in TAW (2001).

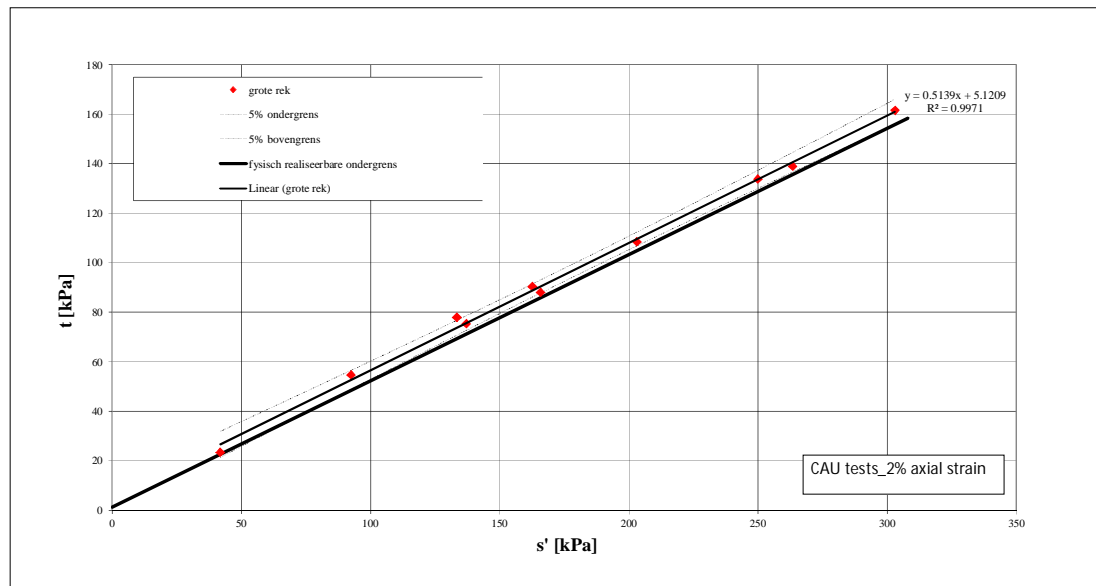


*Figure 3.8* Average, 5% lower/upper confidence limit and physically realizable lower limit t-s' lines for normally consolidated CAU tests at 2% axial strain

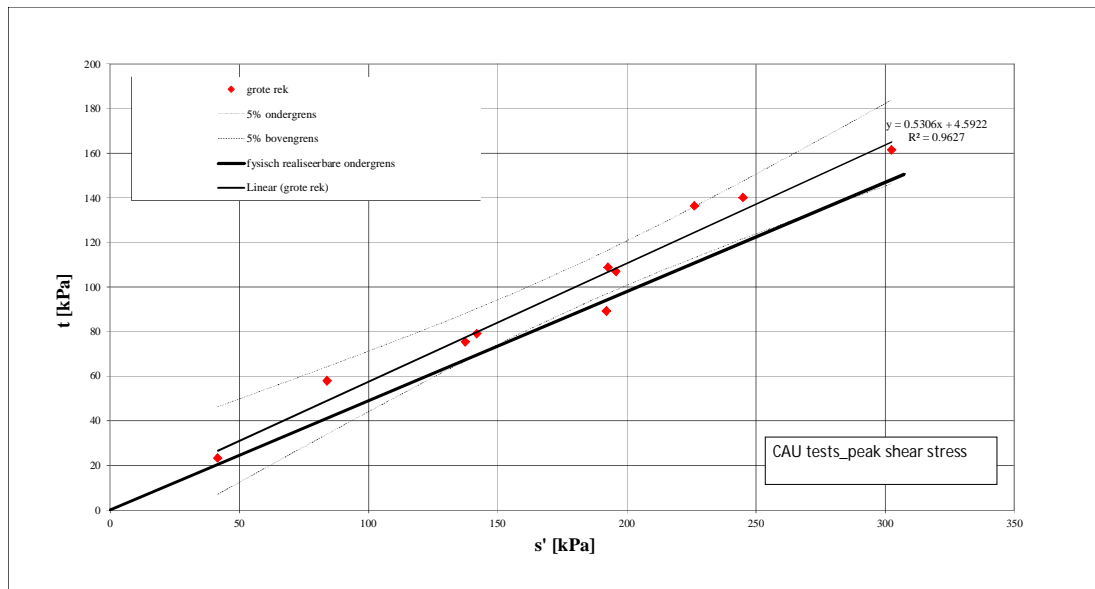


Figure 3.9 Average, 5% lower/upper confidence limit and physically realizable lower limit  $t$ - $s'$  lines for normally consolidated CAU tests at peak shear stress

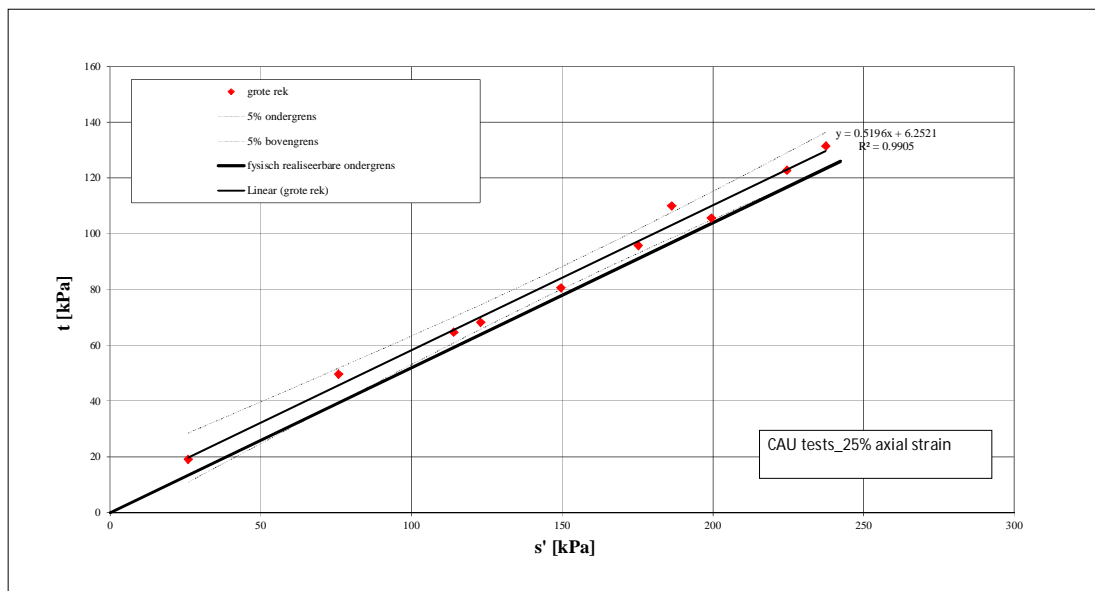


Figure 3.10 Average, 5% lower/upper confidence limit and physically realizable lower limit  $t$ - $s'$  lines for normally consolidated CAU tests at 25% axial strain

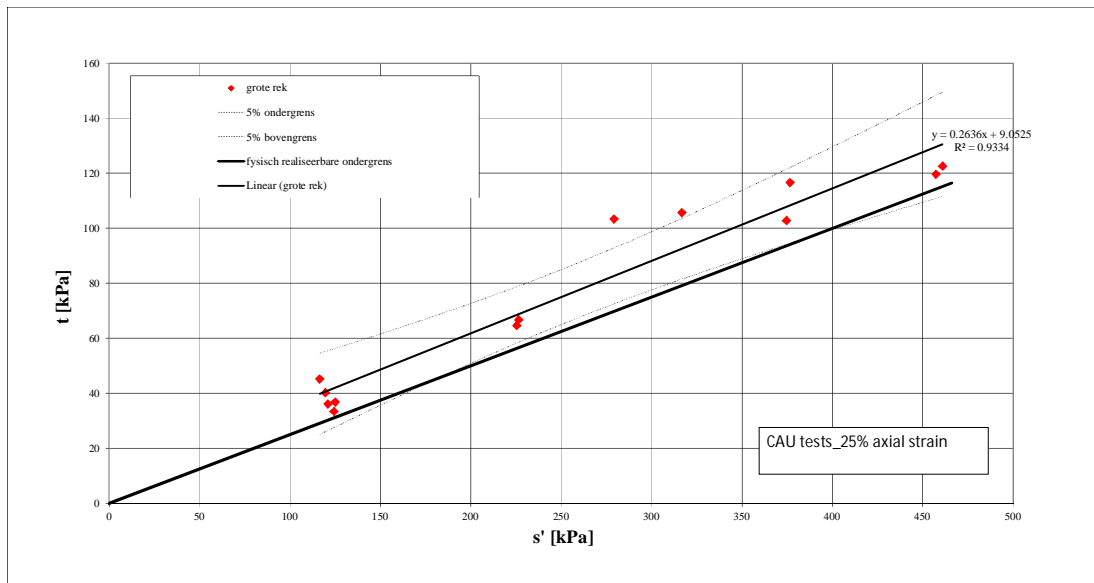


Figure 3.11 Average, 5% lower/upper confidence limit and physically realizable lower limit  $t$ - $s'$  lines for normally consolidated DSS tests at 5% shear strain

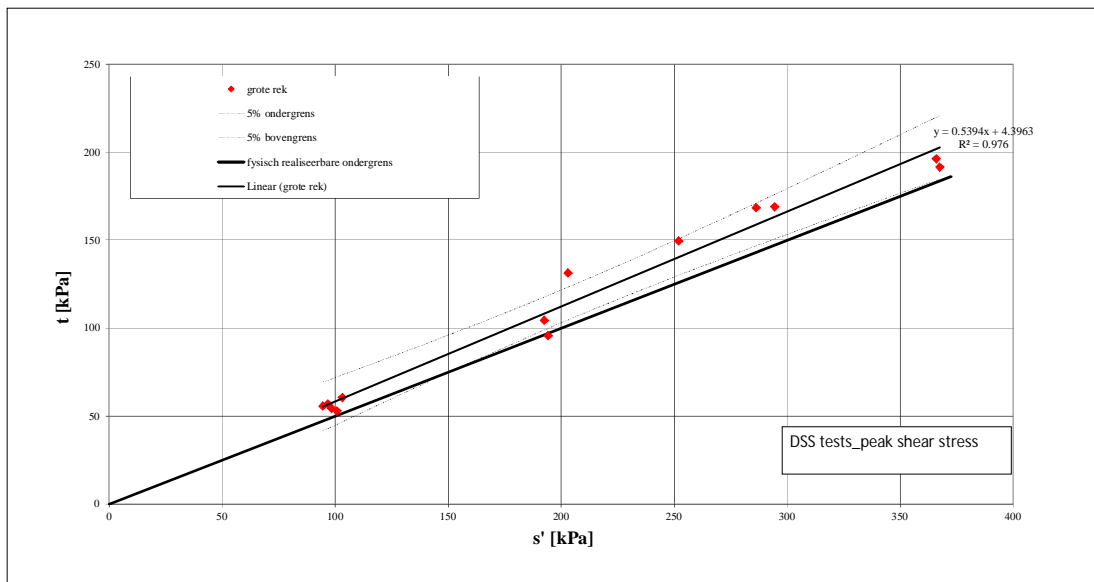


Figure 3.12 Average, 5% lower/upper confidence limit and physically realizable lower limit  $t$ - $s'$  lines for normally consolidated DSS tests at peak shear stress

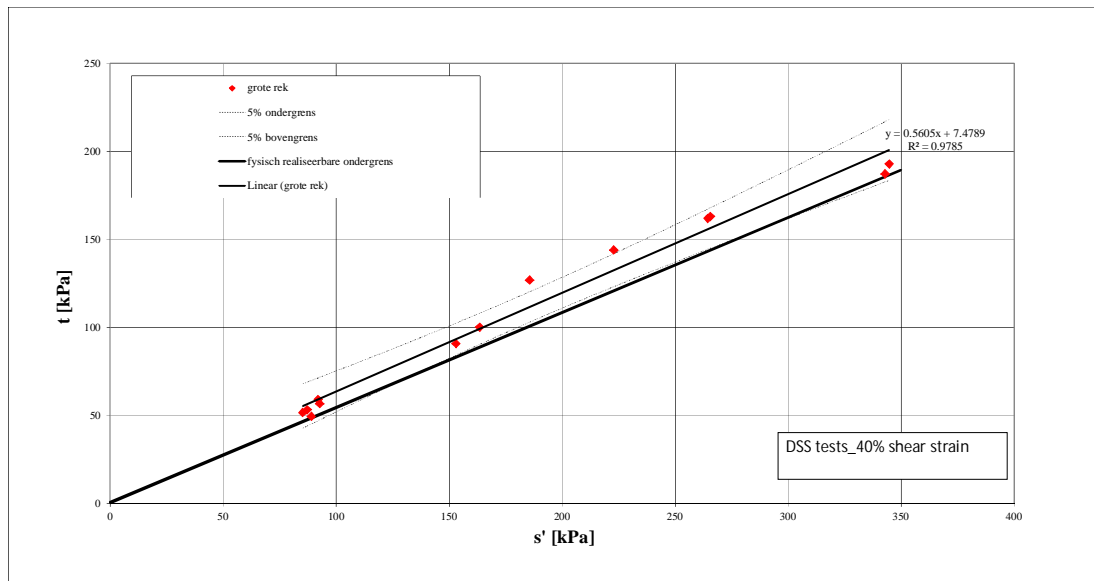


Figure 3.13 Average, 5% lower/upper confidence limit and physically realizable lower limit  $t$ - $s'$  lines for normally consolidated DSS tests at 40% shear strain

For some occasions the calculated 5% lower confidence limit resulted in negative  $c'_{kar}$  – cohesion values. In these cases the characteristic value,  $c'_{kar,}$  was taken equal to zero while the  $\phi'_{kar}$  value was adjusted so that the produced data ('physically realizable lower limit' line) fit as closely as possible the 5% lower confidence limit line (refer to Figure 3.9, Figure 3.10 and Figure 3.12).

For the shear strength parameters the local, average standard deviation,  $\sigma_{loc,aver}$ , and the standard deviation of the regional variation,  $\sigma_{reg}$ , for a normal data distribution are listed in Table 3.6 below. In this table the relevant average values of the shear strength parameters are also presented.

Type of test	Testing Phase	$\tan\phi' [-]$			c [kPa]		
		Average	$\sigma_{reg}$	$\sigma_{loc,aver}$	Average	$\sigma_{reg}$	$\sigma_{loc,aver}$
CAU	Peak	0.62	0.07	0.04	5.42	4.92	2.91
	2% shear strain	0.6	0.01	0.01	5.97	4.11	2.43
	25% shear strain	0.61	0	0	7.32	6.65	3.94
DSS	Peak	0.54	0.05	0.03	4.4	4.28	2.45
	5% shear strain	0.26	0.02	0.01	9.05	8.8	5.03
	40% shear strain	0.56	0.03	0.02	7.48	6.88	3.94

Table 3.6: Standard deviation of the shear strength parameters – Normal data distribution

3.1.6 Assessment of undrained Young's Modulus, E and shear modulus, G  
 The undrained Young's modulus, E, was calculated directly from the stress-strain paths of the available triaxial tests as these were performed under undrained testing conditions.

The undrained Young's modulus ( $E_{u,50}$ ) and the shear modulus ( $G_{50}$ ) were calculated at 50% of the peak shear stress (Wood, 1990).

The drained Young's modulus values have been calculated via the equation:

$$E'_{50} = \frac{E_{u,50} \cdot (1 + \nu')}{(1 + \nu_u)} \quad (7)$$

Where:

- $E_{u,50}$  is the undrained Young's modulus at 50% of the peak shear strength;
- $E'_{50}$  is the drained Young's modulus at 50% of the peak shear strength;
- $\nu_u$  is the Poisson's ratio for undrained conditions and
- $\nu'$  is the Poisson's ratio for drained conditions.

The undrained value of Poisson's ratio  $\nu_u = 0.5$ . Typical values of drained Poisson's ratio fall in the range  $0.1 < \nu' < 0.3$ . For the purposes of this analysis an average value of  $\nu' = 0.2$  is used as assessed from the Ko-CRS tests performed on clay samples (see  $\nu_{ur}$  values in *Table 3.4*).

The calculated  $E_{u,50}$ ,  $E'_{50}$  and  $G_{50}$  values can be seen in *Table 3.7* and *Table 3.8* for the case of CAU and DSS tests respectively.

a/a	Test ID	Sample Depth [NAP m]	Raai	Boring	Location	$t_c$ (kPa)	$t_{peak}$ (kPa)	$E_{u,50}$ (MPa)	$E'_{50}$ (MPa)	Test Conditions	Type of soil based on the geological profile	Lab
1	M011	-0.78	1	B103	K	17.9	50.3	4.63	3.70	in situ	Klei met schelpen	W
2	M013	-2.02	1	B103	K	21.2	67.9	4.99	3.99	in situ	Klei met schelpen	W
3	M015	-2.89	1	B103	K	102.7	140.2	69.8	55.80	NC	Klei met schelpen	W
4	M017	-3.78	1	B103	K	102.3	136.4	31.1	24.87	NC	Klei met plantenresten	W
5	M019	-5.01	1	B103	K	24.3	54.8	11.3	9.05	in situ	Klei met plantenresten	W
6	M023	-6.99	1	B103	K	28.7	74	7.67	6.14	in situ	Klei met plantenresten	W
7	M025	-8	1	B103	K	31.6	73	6.65	5.32	in situ	Klei met plantenresten	W
8	M003	-1.92	1	B104	A	5.2	23.5	3.04	2.43	in situ	Klei met schelpen	W
9	M005	-3.03	1	B104	A	37.3	58	11.6	9.30	NC	Klei met schelpen	W
10	M009	-5.09	1	B104	A	9.5	27.5	1.36	1.09	in situ	Klei met plantenresten	W
11	M010	-5.38	1	B104	A	11.0	23	3.3	2.64	in situ	Klei met plantenresten	W
12	M015	-8.07	1	B104	A	18.0	29.7	8.77	7.02	in situ	Klei met plantenresten	W
13	M018	-9.65	1	B104	A	25.4	45.7	4.48	3.58	in situ	Klei met plantenresten	W
14	M007	-0.47	2	B203	K	18.4	50.4	12.9	10.30	in situ	Klei_antropogeen	W
15	M011	-2.51	2	B203	K	124.7	161.6	73.2	58.57	NC	Klei met plantenresten	W
16	M013	-3.62	2	B203	K	22.9	47.7	7.89	6.31	in situ	Klei met plantenresten	W
17	M014	-3.93	2	B203	K	23.2	39.1	9.22	7.38	in situ	Klei met plantenresten	W
18	M004	-2.35	2	B204	A	6.6	23.5	2.09	1.67	in situ	Klei met schelpen	W
19	M005	-2.78	2	B204	A	54.3	75.5	34.5	27.60	NC	Klei met schelpen	W
20	M008	-4.2	2	B204	A	11.3	32.7	2.83	2.26	in situ	Klei met plantenresten	W
21	M010	-5.11	2	B204	A	14.3	40.2	3.83	3.06	in situ	Klei met plantenresten	W
22	M017	-8.6	2	B204	A	24.2	57.1	3.96	3.17	in situ	Klei met plantenresten	W
23	M005	0.23	4	B401	K	61.9	107	16.7	13.33	NC	Klei_antropogeen	W
24	M007	-0.57	4	B401	K	16.1	54.4	6.53	5.22	in situ	Klei_antropogeen	W
25	M008	-1.08	4	B401	K	16.9	44.7	5.2	4.16	in situ	Klei met schelpen	W
26	M010	-2.09	4	B401	K	19.1	55.1	8.52	6.82	in situ	Klei met schelpen	W
27	M013	-3.82	4	B401	K	21.6	53.5	7.6	6.08	in situ	Klei met plantenresten	W
28	M014	-4.27	4	B401	K	85.5	108.9	73.9	59.08	NC	Klei met plantenresten	W
29	M001	-3.5	4	B404	A	17.2	23.4	8.32	6.66	NC	Klei met plantenresten	W
30	M002	-4.58	4	B404	A	5.0	18.6	0.9	0.72	in situ	Klei met plantenresten	W
31	M004	-5.49	4	B404	A	6.4	20.1	1.28	1.02	in situ	Klei met plantenresten	W
32	M016	-11.61	4	B404	A	15.4	29.2	3.87	3.10	in situ	Klei met plantenresten	W
33	M018	-12.65	4	B404	A	18.1	29.3	6.7	5.36	in situ	Klei met plantenresten	W
34	M013	-8.05	5	B504	A	17.1	26.8	6.6	5.28	in situ	Klei met plantenresten	W
35	M003	-3.01	5	B504	A	8.5	36.9	4.95	3.96	in situ	Klei met plantenresten	W
36	M002	-2.64	5	B504	A	63.8	79.2	45.7	36.55	NC	Klei met schelpen	W
37	M015	-4.78	5	B503	K	19.4	43.8	8.04	6.43	in situ	Klei met plantenresten	W
38	M009	-1.71	5	B503	K	16.5	64.1	8.59	6.87	in situ	Klei met schelpen	W
39	M007	-0.73	5	B503	K	72.2	89.3	83.8	67.04	NC	Klei met schelpen	W
40	M006a	-0.13	5	B503	K	14.8	40.3	5.14	4.11	in situ	Klei_antropogeen	W
41	M011a	-0.83	1	B103	K	17.7	56.1	5.5	4.40	in situ	Klei met schelpen	D
42	M003a	-1.97	1	B104	A	4.4	18.9	1.5	1.20	in situ	Klei met schelpen	D
43	M007a	-0.53	2	B203	K	17.1	45.2	4.5	3.60	in situ	Klei_antropogeen	D
44	M008a	-4.27	2	B204	A	11.3	34.8	2.6	2.08	in situ	Klei met plantenresten	D
45	M004a	-5.57	4	B404	A	6.3	19.1	1.4	1.12	in situ	Klei met plantenresten	D
46	M006a	-0.19	5	B503	K	14.5	34.2	3.5	2.80	in situ	Klei_antropogeen	D
47	M009a	-1.5	5	B503	K	16.4	47.8	9	7.20	in situ	Klei met schelpen	D

Where:  $t_c$  is the shear stress at the end of the anisotropic consolidation;  $t_{peak}$  is the peak shear stress;  $E_{u,50}$  is the undrained Young's modulus at 50% of the peak shear strength;  $E'_{50}$  is the drained Young's modulus at 50% of the peak shear strength; A = Achterland; K = Kruijn; W = Wiertsema and D = Deltares.

Table 3.7 Summary of Young's modulus  $E_{50}$  values for the CAU tests performed



a/a	Test ID	Raai	Boring	Location	$\tau_{peak}$ (kPa)	$G_{50}$ (MPa)	Direction of loading	Testing Conditions	Type of soil based on the geological profile	Lab
1	M021-A	1	B103	K	168.5	2.41	⊥	NC	Hollandveen	W
2	M021-B	1	B103	K	168.9	3.14	//	NC	Hollandveen	W
3	M006-A	1	B104	A	54.5	1.28	⊥	NC	Hollandveen	W
4	M006-B	1	B104	A	52.9	1.02	//	NC	Hollandveen	W
5	M018-A	2	B203	K	191.6	3.11	⊥	NC	Hollandveen	W
6	M018-B	2	B203	K	196.3	2.83	⊥	NC	Hollandveen	W
7	M019-A	2	B203	K	74.5	1.56	⊥	In situ	Hollandveen	W
8	M019-B	2	B203	K	69.8	1.34	//	In situ	Hollandveen	W
9	M011-A	2	B204	A	95.8	1.74	⊥	NC	Hollandveen	W
10	M011-B	2	B204	A	104.4	1.66	//	NC	Hollandveen	W
11	M014-A	2	B204	A	43.5	0.83	⊥	In situ	Hollandveen	W
12	M014-B	2	B204	A	41.5	0.93	//	In situ	Hollandveen	W
13	M007-A	4	B404	A	60.5	0.96	⊥	NC	Hollandveen	W
14	M007-B	4	B404	A	57	0.80	//	NC	Hollandveen	W
15	M008-A	4	B404	A	22.7	0.36	⊥	In situ	Hollandveen	W
16	M008-B	4	B404	A	22.9	0.38	//	In situ	Hollandveen	W
17	M010-A	4	B404	A	26.8	0.51	⊥	In situ	Hollandveen	W
18	M010-B	4	B404	A	25.2	0.45	//	In situ	Hollandveen	W
19	M010-A	5	B503	K	61.3	1.55	⊥	In situ	Hollandveen	W
20	M010-B	5	B503	K	57.4	1.49	//	In situ	Hollandveen	W
21	M017-A	5	B503	K	149.5	2.79	⊥	NC	Hollandveen	W
22	M017-B	5	B503	K	131.3	3.26	//	NC	Hollandveen	W
23	M004-A	5	B504	A	55.8	2.07	⊥	NC	Hollandveen	W
24	M005-A	5	B504	A	21.4	0.36	⊥	In situ	Hollandveen	W
25	M005-B	5	B504	A	21.7	0.41	//	In situ	Hollandveen	W
26	M006-A	5	B504	A	21.4	0.46	⊥	In situ	Hollandveen	W
27	M006-B	5	B504	A	20.2	0.30	//	In situ	Hollandveen	W
28	M009-A	5	B504	A	25.3	0.39	⊥	In situ	Hollandveen	W
29	M009-B	5	B504	A	23.7	0.39	//	In situ	Hollandveen	W
30	M018b	2	B203	K	79.5	1.21	⊥	In situ	Hollandveen	D
31	M010a	2	B203	K	57.2	0.98	⊥	In situ	Hollandveen	D
32	M020a	2	B203	K	73.1	1.15	⊥	In situ	Hollandveen	D
33	M012b	5	B503	K	54.9	0.79	⊥	In situ	Hollandveen	D
34	M004b	5	B504	A	18.1	0.02	⊥	In situ	Hollandveen	D
35	M017b	5	B503	K	59	0.78	⊥	In situ	Hollandveen	D
36	M004c	5	B504	A	23.1	0.40	//	In situ	Hollandveen	D
37	M021b	1	B103	K	70.3	1.10	//	In situ	Hollandveen	D

Where  $\tau_{peak}$  is the peak shear stress and  $G_{50}$  is the shear modulus at 50% of the peak shear strength.

Table 3.8 Summary of the shear modulus  $G_{50}$  for the DSS tests performed

A stress level dependency of the  $E_{50}$  and  $G_{50}$  values can be observed in Figure 3.14 and Figure 3.15 which presents the  $E_{50}$  and  $G_{50}$  values respectively as a function of the applied effective vertical stress at the end of consolidation for the tests performed both at in situ and normally consolidated conditions.

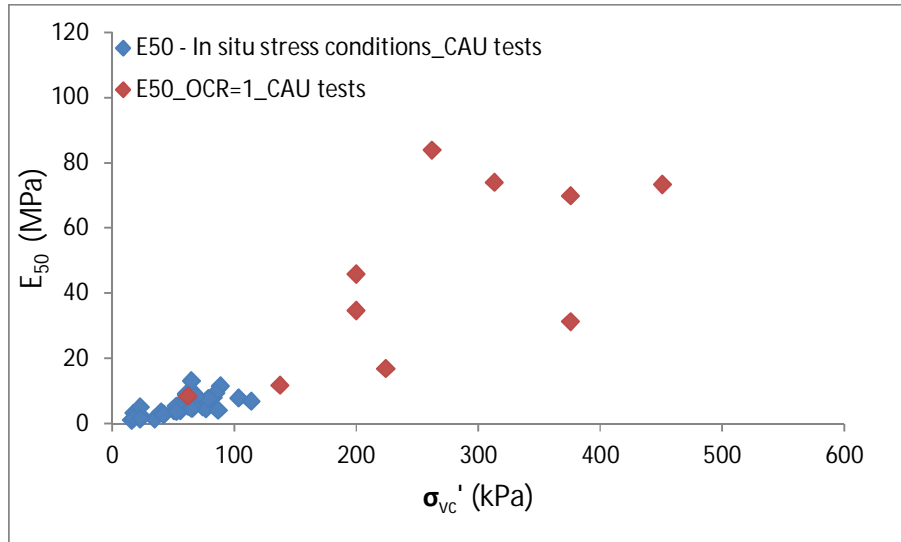


Figure 3.14 Stress level dependency of the  $E_{50}$  values for the tests performed at in situ and normally consolidated conditions

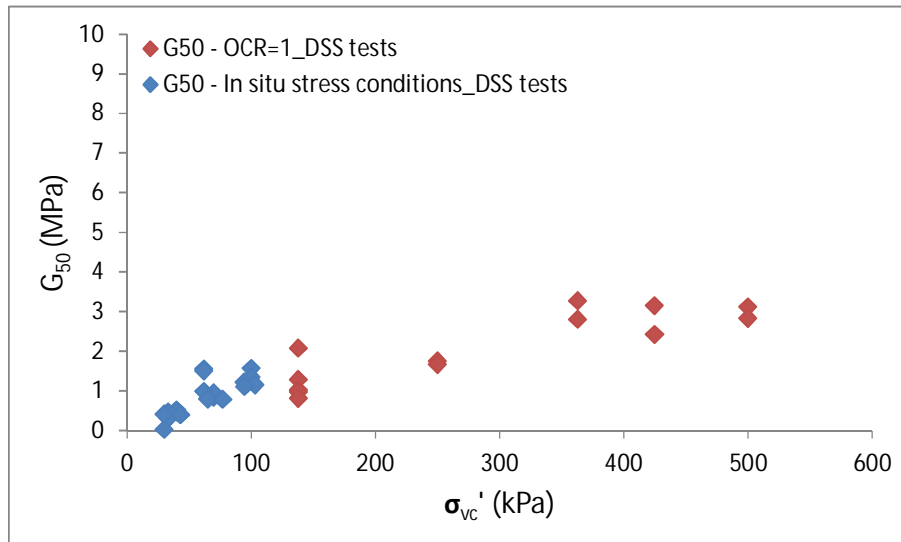


Figure 3.15 Stress level dependency of the  $G_{50}$  values for the tests performed at in situ and normally consolidated conditions

To account for the observed stress level dependency of the Young's modulus the data is normalized with respect to a reference stress of 10 kPa ( $p^{ref} = 10 \text{ kPa}$ ) and plotted in a Young's modulus versus  $\sigma'_3/p^{ref}$  graph (where  $\sigma'_3$  is the minor principal stress at the end of

the consolidation) for samples tested at in situ stress conditions (Figure 3.16) and for samples tested at normally consolidated conditions (Figure 3.17).

The stress dependent stiffness modulus can be given by the following equation:

$$E_{50} = E_{50}^{Ref} \left( \frac{\sigma_3'}{p^{Ref}} \right)^m \quad (8)$$

Where:

- $m$  = power for stress level dependency of stiffness
- $p^{ref}$  = reference stress level (=10kPa) and
- $E_{50}^{Ref}$  = reference stiffness modulus corresponding to the reference pressure  $p^{ref}$ .

Based on Eq. (8) the  $E_{50}^{Ref}$  and  $m$  values are graphically calculated from Figure 3.17 as follows:

- For in situ stress conditions  
 $E_{50}^{Ref} = 2.04 \text{ MPa}$   
 $m = 0.97$
- For normally consolidated conditions  
 $E_{50}^{Ref} = 2.78$   
 $m = 1.1$

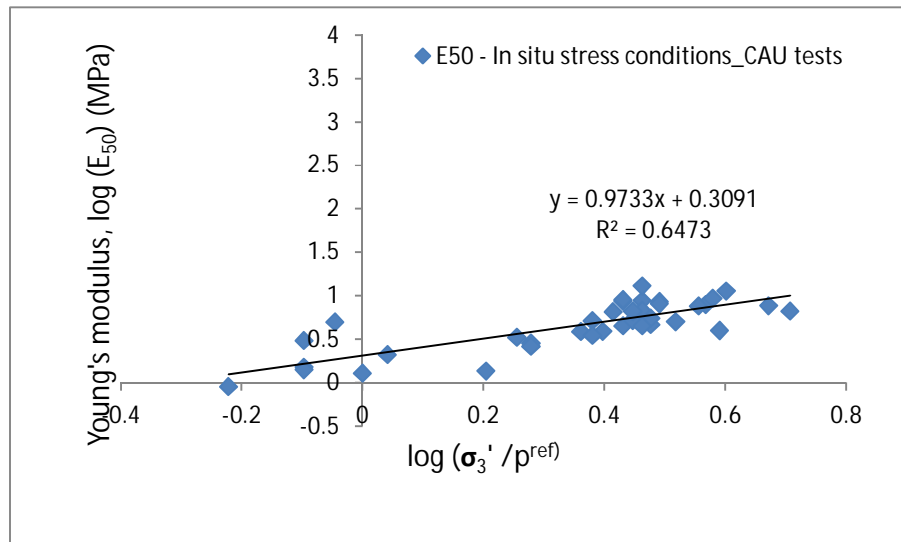


Figure 3.16 Stress level dependency of  $E_{50}$  and  $G_{50}$  values for tests performed at in situ stress conditions; use of bi-logarithmic scale

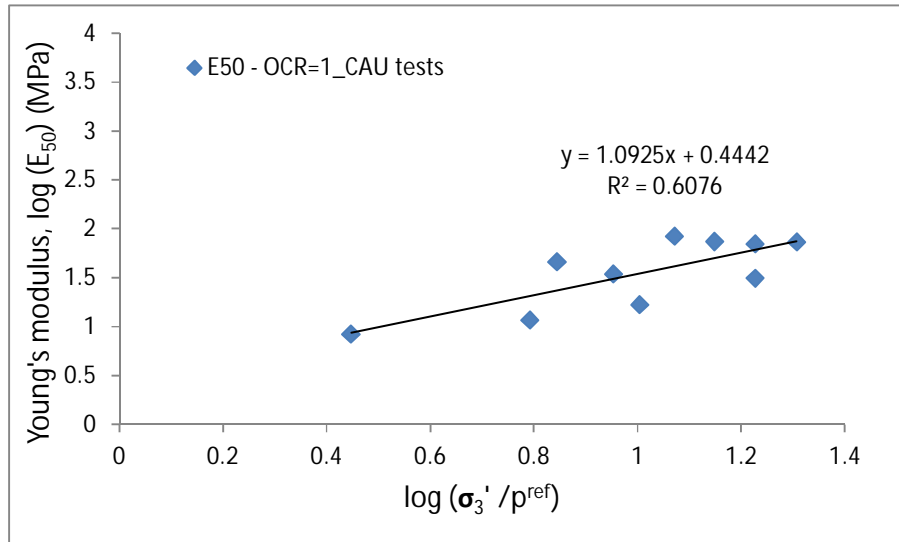


Figure 3.17 Stress level dependency of  $E_{50}$  values for tests performed at normally consolidated conditions ( $OCR=1$ ); use of bi-logarithmic scale

The Shansep model analysis calculations require as input a constant value of the ratio of shear modulus  $G$  over the undrained shear strength,  $s_u$ . The input parameter,  $G/s_u$ , allows to model the increase of stiffness with depth and thereby its variation with the current effective stress state. Figure 3.18 and Figure 3.19 illustrate the distribution of this ratio as a function of OCR for the case of the clay and peat samples of this study respectively. For peat an average value of  $G_{50}/s_u = 20.5$  can be considered.

For the case of the clay samples the  $E_{50}$  values have been converted to  $G_{50}$  values via the relationship:

$$G_{50} = \frac{E_{50}}{2(1 + \nu_u)} \quad (9)$$

For the undrained testing conditions  $\nu_u=0.5$  and Eq. (9) is simplified to:

$$G_{50} = \frac{E_{50}}{3} \quad (10)$$

For the clay samples a large scatter of the data can be observed for  $OCR = 1$ . This behaviour might be attributed to the different plasticity index values of the tested soil specimens. The ratio  $G_{50}/s_u$  for the clay samples tested under normally consolidated conditions is plotted versus the plasticity index,  $I_p$  in Figure 3.20. The Termaat, Vermeer and Vergeer (1985)  $G_{50}/s_u - I_p$  fitting line for normally consolidated clays is also presented for comparison. With the exception of the test data at  $OCR=1$ , an average value of  $G_{50}/s_u=60$  can be considered for the case of clay samples. As can be seen in Figure 3.18, this value appears to be in agreement with the Seah & Lai (2003) fitting line derived from triaxial compression test data on soft Bangkok clay samples.

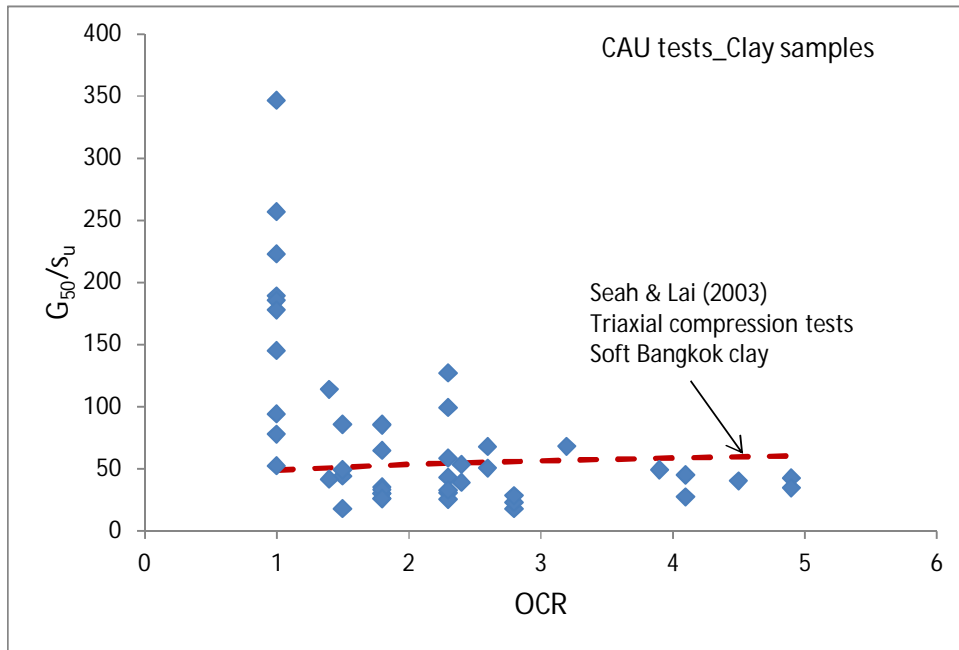


Figure 3.18 Variation of  $G_{50}/s_u$  ratio with OCR; clay samples

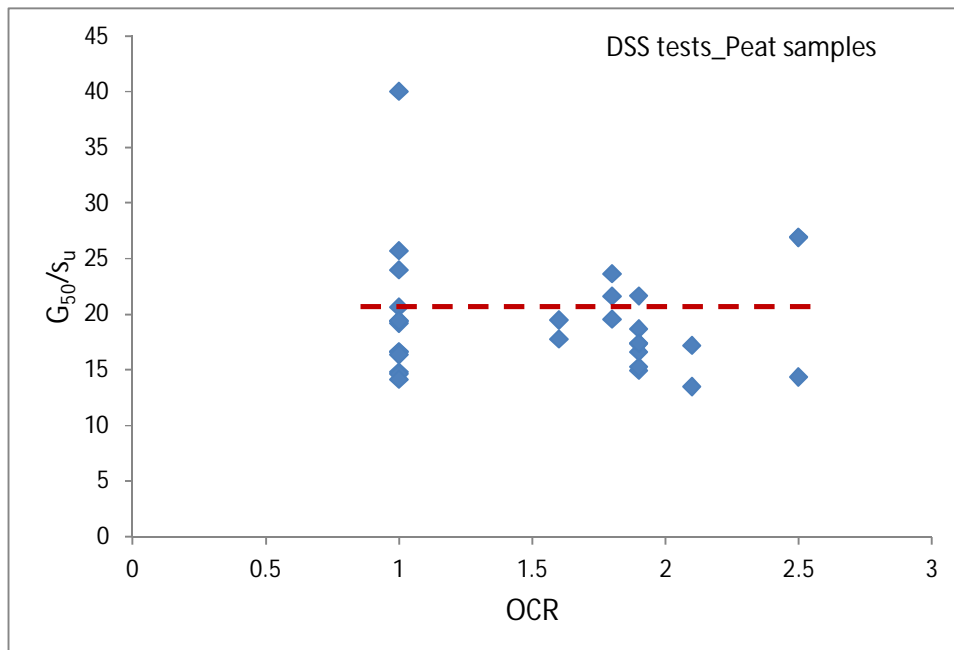


Figure 3.19 Variation of  $G_{50}/s_u$  ratio with OCR; peat samples

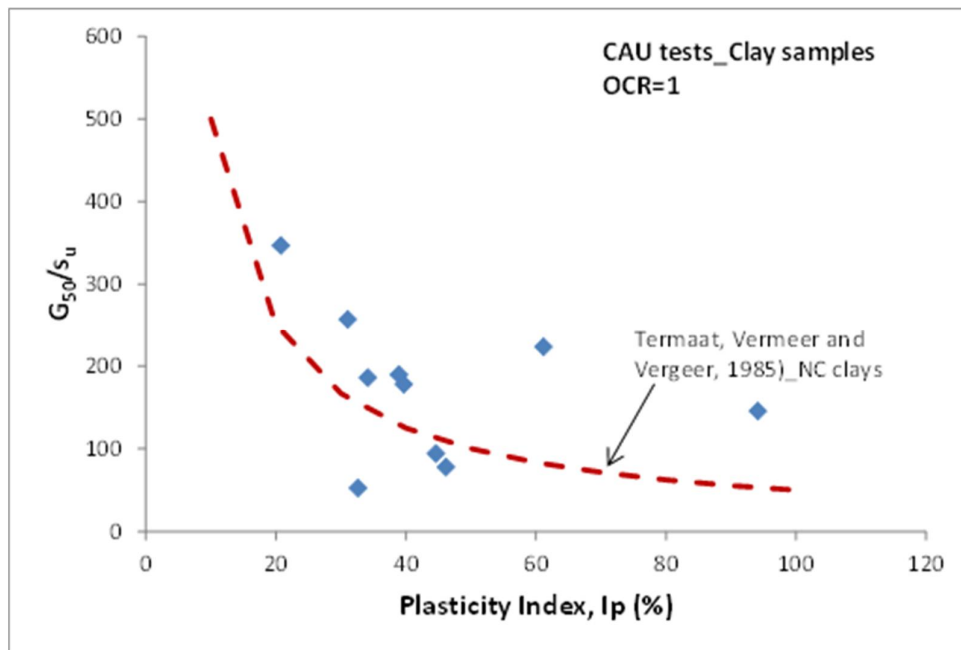


Figure 3.20 Variation of  $G_{50}/s_u$  ratio with plasticity index,  $I_p$ ; clay samples with  $OCR=1$

### 3.1.7 LDSS test results

Peat generally consists of long fibres and the effect of this structure on the material's strength properties might not be fully captured by the performance of small scale tests. To assess whether there is an influence of the size of the tested samples on the strength properties of the peat material under consideration the conventional DSS tests of this study were supplemented with LDSS tests. The DSS tests were performed on cylindrical samples with an initial height and diameter of approximately 20 mm and 63 mm respectively while for the LDSS tests rectangular samples with dimensions of 260 mm (length) x 220 mm (width) x 80 mm (height after consolidation) were tested.

The LDSS stress paths for the four tests performed are shown in Figure 3.21.

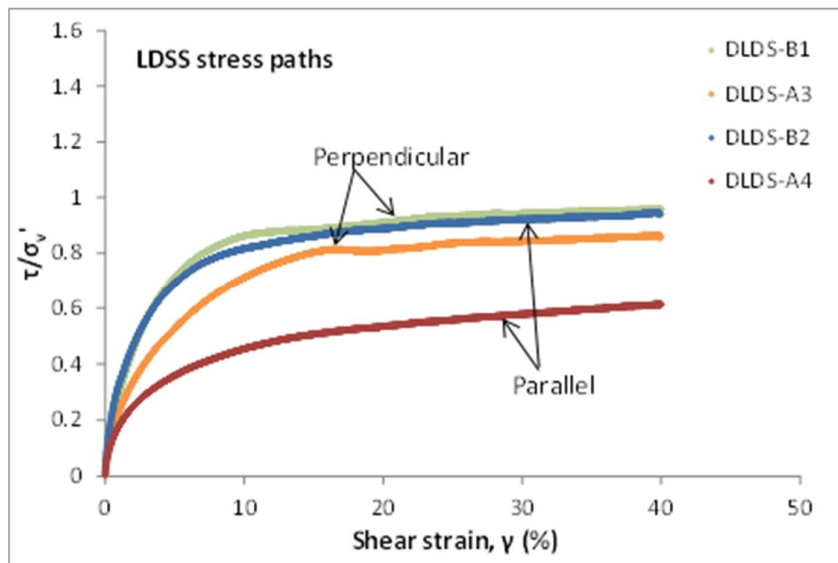


Figure 3.21 Normalized stress paths of LDSS tests

An insight on the geological formation of the peat samples tested and the failure scheme after shearing is provided in Figure 3.23 to Figure 3.26. In these figures photos of the samples after termination of the shearing and before removal from the apparatus are shown. Prior to testing the peat samples were described by an expert geologist while soil classification tests, water content,  $w$ , particle density,  $\rho_s$  and Loss On Ignition, LOI tests, were performed. The results of these tests together with the geological description of each sample are summarized in Appendix I. For visual purposes these results are also illustrated in Figure 3.22. The peat samples from boring DLDS-B have a more clayish structure as this is reflected in the lower water content ( $WC_{average} \approx 179\%$ ), higher particle density ( $\rho_s \approx 20.6 \text{ kN/m}^3$ ), and lower organic content values ( $OC_{average} \approx 33\%$ ) obtained compare to the samples from boring DLDS-A with values of  $WC_{average} \approx 483\%$ ,  $\rho_s \approx 15.6 \text{ kN/m}^3$  and  $OC_{average} \approx 78\%$ . Thus, the base of comparison of the LDSS test results should be limited to samples from the same boring location. According to this perspective, it can be concluded from Figure 3.21 that the stress paths for the samples from boring DLDS-B (DLDS-B1 & DLDS-B2) appear to converge, resulting in approximately similar values of peak/large strain shear stress. The behaviour of samples from boring DLDS-A (DLDS-A3 & DLDS-A4) exhibit significant differences when compared to each other with sample DLDS-A4 showing lower shear stress ratio values for the range of shear strains applied.

Based on visual observations in the lab sample DLDS-A4 has different soil texture characteristics in comparison to sample DLDS-A3. The material of sample DLDS-A4 has a rather softer structure, an observation in agreement with the relatively high strain values at the end of its consolidation stage. Specifically, the consolidation strain receives a value of 4.1%, 3.4%, 6.9% and 18.8% for the samples DLDS-B1, DLDS-B2, DLDS-A3 and DLDS-A4 respectively. The difference in the texture characteristics of sample DLDS-A4 can explain to some extent its weaker stress path behaviour shown in Figure 3.21.

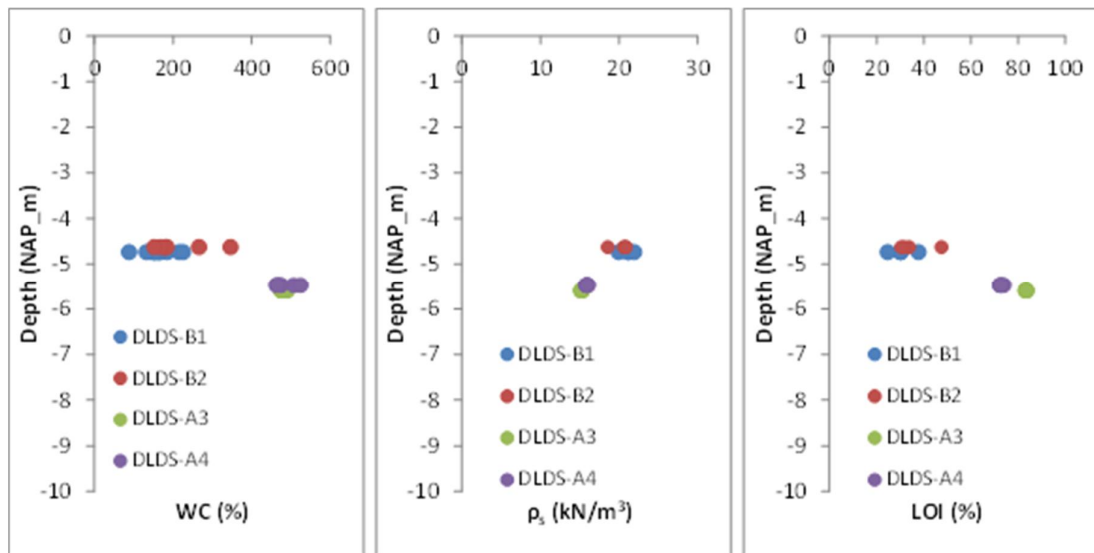


Figure 3.22 In depth profile of water content, particle density and LOI for the LDSS tests performed

A comparison of the LDSS stress paths with those of samples tested under DSS conditions is provided in Figure 3.27 and Figure 3.28. To eliminate the influence of consolidation level on the comparison of the test results the shear stress,  $\tau$ , has been normalized with respect to the effective vertical stress at the end of consolidation. Figure 3.27 presents the LDSS and DSS test results for samples subjected to shearing with the direction of loading perpendicular to the direction of the dike while Figure 3.28 presents the test results for the case of loading parallel to the direction of the dike. The comparison of the test results in terms of  $\tau_{peak}/\sigma_v'$  and  $\tau_{40\%}/\sigma_v'$  ratios is shown in Figure 3.29 and Figure 3.30 respectively. The DSS samples presented in Figure 3.27 to Figure 3.30 where retrieved from Raai 5 and Boring 504 (Boring co-ordinates: X = 108213.70, Y = 445988.20 and Z = NAP -1.30 m). The two borings from where the LDSS samples were retrieved from originated from adjacent locations to Boring B504. Specifically the co-ordinates of these borings are as follows:

Boring ID: DLDS-A; X = 108214, Y=445986.6, Z = NAP -1.33 m

Boring ID: DLDS-B; X = 108214.8, Y=445988.7, Z = NAP -1.39 m

LDSS tests were performed on samples with testing depths relatively similar to the depths of the DSS samples (LDSS depth range: -3.24 m to -4.27 m NAP; DSS depth range: -4.08 m to -6.12 m NAP). The depth at the top of each tested sample is noted in the legend of Figure 3.27 and Figure 3.28. The distribution of the OCR values within the above depth ranges (refer to Figure 3.7) indicate that DSS and LDSS samples with a rather identical stress history are compared in Figure 3.29 and Figure 3.30.





Figure 3.23 Test ID: DLDS -B1\_Photos of the sample after shearing, during removal from the apparatus



Figure 3.24 Test ID: DLDS -B2\_Photos of the sample after shearing, during removal from the apparatus



Figure 3.25 Test ID: DLDS -A3\_Photos of the sample after shearing, during removal from the apparatus



Figure 3.26 Test ID: DLDS -A4\_Photos of the sample during trimming and after shearing, during removal from the apparatus

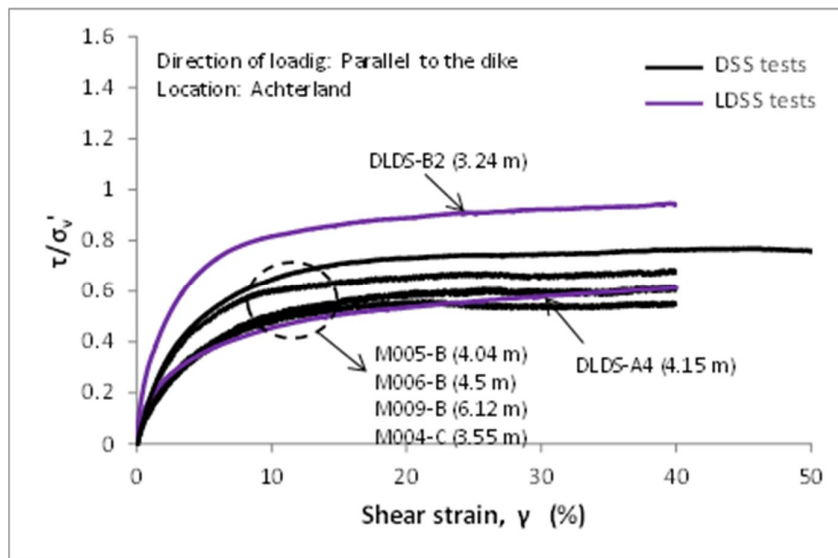


Figure 3.27 Normalized stress paths of LDSS and DSS tests; loading perpendicular to the dike

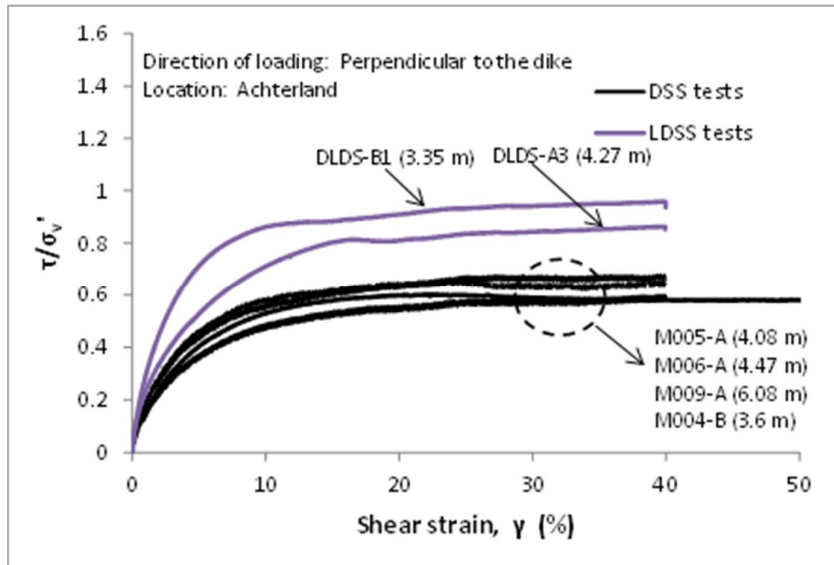


Figure 3.28 Normalized stress paths of LDSS and DSS tests; loading parallel to the dike

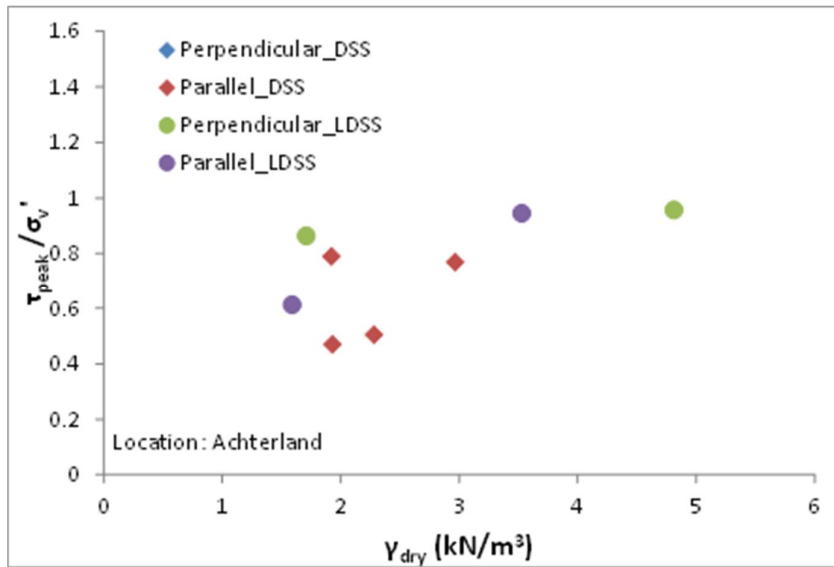


Figure 3.29 Distribution of  $\tau_{peak}/\sigma'_v$  ratio with samples' dry density



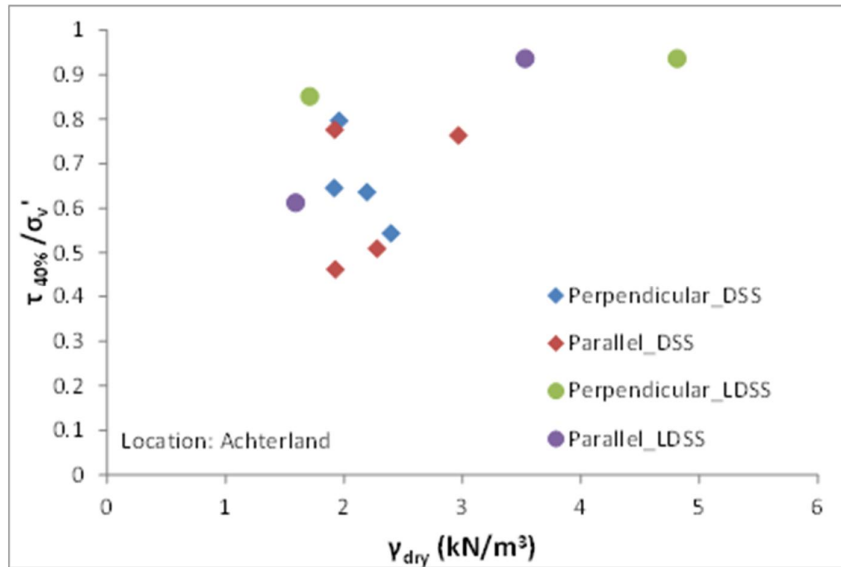


Figure 3.30. Distribution of  $\tau_{40\%} / \sigma_v'$  ratio with samples' dry density

Geological description shows that the LDSS samples mainly consist of organic debris including some anthropogenic artefacts, bone fragments, leather and pieces of pottery. Extra hand augers were made for further sub soil inspection and showed the presence of an old ditch filled organic material. The results of the hand augers are discussed in companion report, 1220518-005-GEO-0003. The large samples appeared to be taken from this ditch filling and are therefore believed to differ from the conventional samples taken from the peat layer. The difference in nature makes it difficult to conclude about the comparison between the LDSS tests and the conventional tests. To benefit from the potential positive influence of the LDSS results it is recommended to take extra samples, from the peat layer and do additional tests. When disregarding the differences between the LDSS samples and the conventional samples, the following conclusions can be drawn:

(a) Effect of the direction of loading

As aforementioned, to assess the influence of the direction of loading for each boring location a pair of samples was tested at adjacent depths with one of the samples subjected to perpendicular to the dike loading direction and the other one to parallel to the dike direction of loading. For the pair of samples from boring DLDS-A (DLDS-A3 & DLDS-A4) the difference in the soil texture characteristics among the two tested samples do not allow their direct comparison and therefore no conclusions can be drawn on the effect of the direction of loading on the samples' response. For the pair of samples from boring DLDS-B (DLDS-B1 & DLDS-B2) the stress path behaviour is practically identical (refer to Figure 3.21) independently of the direction of loading supporting the findings of the conventional DSS tests which show no apparent influence of the direction of loading on the undrained shear strength behaviour of the tested samples.

(b) Comparison of LDSS and DSS test results

With the exception of test LDSS-A4 (for reasons discussed above), the general pattern observed is obtaining higher shear stress ratio values for samples tested

under LDSS conditions compare to the samples tested under DSS conditions for the same strain levels. In particular, the shear stress ratio at peak and at 40% shear strain can be increased by a factor of 44% (factor estimated based on the average shear stress ratio values of the DSS and LDSS tests). It is believed that testing in a larger scale represents in situ soil behaviour more accurately as it accommodates in a better degree the spectrum of encountered soil features. According to this, the current interpretation of the test results implies that the use of the DSS shear stress values as input in FEM and LEM analysis calculations can be considered as a rather conservative approach.

### 3.2 In situ test results

#### 3.2.1 General

In this section of the report the estimation of the undrained shear strength from in situ tests is assessed. For this purpose the correlation of the laboratory undrained shear strength and tip resistance measurements from cone and ball penetrometer tests is evaluated. Empirical cone and ball penetrometer factors were determined per type of soil and type of test while parameter values such as the effective vertical yield stress is interpreted from CPT measurements and presented herein.

#### 3.2.2 Assessment of undrained shear strength

The undrained shear strength,  $s_u$  is estimated from CPT data by using the following correlation with the net cone resistance ( $q_{net}$ ):

$$s_u = \frac{q_{net}}{N_{kt}}$$

$$q_{net} = q_t - \sigma_{vo} \quad (11)$$

$$q_t = q_c + (1 - \alpha) \cdot u_2$$

Where:

- $N_{kt}$  = empirical correlation factor, generally referred to as the cone factor;
- $\sigma_{vo}$  = the total vertical stress;
- $q_t$  = the corrected tip resistance;
- $q_c$  = the CPT tip resistance;
- $u_2$  = the pore pressure measured behind the cone shoulder ( $u_2$  position) and
- $\alpha$  = the cone's alpha factor.

The undrained shear strength,  $s_u$ , for the case of ball penetrometer data can be estimated through the following correlation:

$$s_u = \frac{q_b}{N_b} \quad (12)$$

Where:

- $q_b$  = the ball penetrometer tip resistance and
- $N_b$  = empirical correlation factor, generally referred to as the ball penetrometer factor.

For deriving the  $N_{kt}/N_b$  factors, the undrained shear strength values as defined experimentally from the DSS and CAU tests were correlated with the corresponding  $q_{net}/q_b$  values from cone penetration/ball penetrometer tests at similar depths.

For the complete data set the  $N_{kt}/N_b$  factors were computed via linear regression by fitting the data with the least squares method. The objective is to obtain the values of  $N_{kt}/N_b$  for which the sum of the squares of the residues,  $F_{kt}/F_{ball}$  is minimal:

$$F_{kt} = \sum_i \left( s_{u,i} \frac{N_{kt}}{q_{net,i}} - 1 \right)^2, \quad (13)$$

$$F_{ball} = \sum_i \left( s_{u,i} \frac{N_b}{q_{ball,i}} - 1 \right)^2$$

Where:

- $s_{u,i}$  = the undrained shear strength from laboratory tests at the depth  $i$ ;
- $q_{net,i}$  = the net cone resistance which corresponds to  $s_{u,i}$  and
- $q_{ball,i}$  = the ball penetrometer tip resistance which corresponds to  $s_{u,i}$ .

The uncertainty in the above correlations can be expressed via the coefficient of variation as follows:

$$VC_{N_{kt}} = \sqrt{\frac{\sum_{j=1}^n \left( \frac{s_{u,i} - \frac{q_{net,i}}{N_{kt}}}{\frac{q_{net,i}}{N_{kt}}} \right)^2}{n-1}}, \quad (14)$$

$$VC_{N_b} = \sqrt{\frac{\sum_{j=1}^n \left( \frac{s_{u,i} - \frac{q_{ball,i}}{N_b}}{\frac{q_{ball,i}}{N_b}} \right)^2}{n-1}}$$

Where:

- $VC_{N_{kt}}$  = the coefficient of variation of the difference  $s_u - q_{net}/N_{kt}$ ;
- $VC_{N_b}$  = the coefficient of variation of the difference  $s_u - q_{ball}/N_b$  and
- $n$  = the number of  $q_{net,i} - s_{u,i}$  combinations.

The values of  $N_{kt}$  and  $N_b$  were assessed for each type of encountered soil (clay and peat). DSS and CAU tests were performed solely on peat and clay samples respectively. Thus, the aforementioned factors were determined, for the case of peat soil, via correlation with the

DSS test data (Figure 3.31) and for the case of clay soil via correlation with the CAU test data (Figure 3.32).

Conventional cone CPT tests were performed both at the 'Kruin' and 'achterland' locations while ball penetrometer tests were restricted only to the 'achterland' location. The  $N_{kt}$  factor was assessed via correlation of the  $q_{net}$  values with the experimental  $s_u$  data from the 'kruin' location as indicated with green triangle marks in Figure 3.31 and Figure 3.32. In the same figures, for the assessment of the  $N_b$  factor, the  $q_b - s_u$  values from 'achterland' location are plotted with blue triangle marks. It should be noted that the CPT tests were performed close to the location of the sampling boreholes within an horizontal distance in X or Y direction that doesn't exceed 1 m.

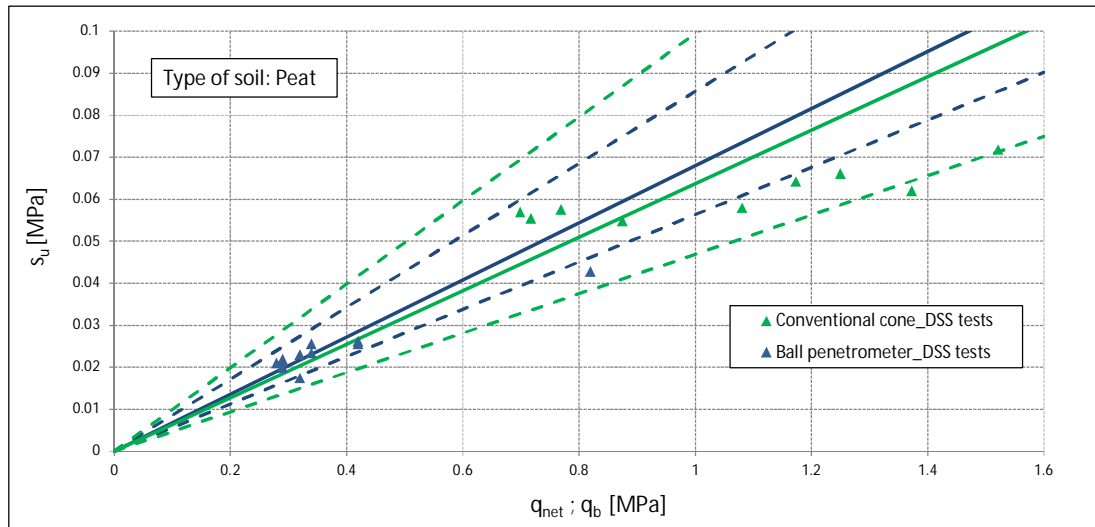


Figure 3.31 Undrained shear strength versus net cone resistance and tip cone resistance; peat soil

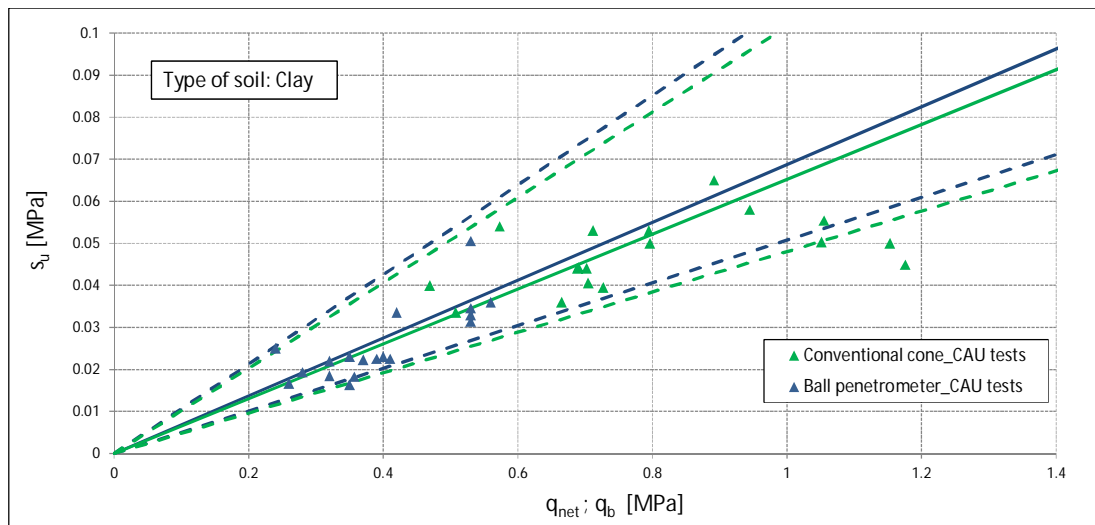


Figure 3.32 Undrained shear strength versus net cone resistance and tip cone resistance; clay soil

The median solid lines in Figure 3.31 and Figure 3.32 correspond to  $N_{kt}$  and  $N_b$  values for which the parameters  $F_{kt}$  and  $F_{ball}$  in Eq. (13) receive minimal values. For these  $N_{kt}$  and  $N_b$  values the 5% lower and upper confidence limit lines are presented in the above figures with dashed lines.

The  $N_{kt}/N_b$  values selected per test type, as calculated from Eq.(13), together with the corresponding VC values, as calculated from Eq.(14), are summarized and presented in *Table 3.9* below.

Type of soil	$N_{kt}$	$VC_{(Nkt)}$	$N_b$	$VC_{(Nb)}$
Peat	15.70	0.218	14.71	0.125
Clay	15.33	0.217	14.55	0.215

*Table 3.9 Cone factors and coefficient of variations for the encountered soils*

### 3.2.3 Assessment of yield stress

The yield stress,  $\sigma'_{vy}$ , of the encountered soil layers is determined according to the following formula:

$$\sigma'_{vy} = \left( \frac{s_u \cdot \sigma'_{vc}{}^m}{\sigma'_{vc} \cdot S} \right)^{\frac{1}{m}} \quad (15)$$

Where:

- $s_u$  = the undrained shear strength;
- $\sigma'_{vc}$  = the effective vertical stress;
- $S$  = the undrained shear strength ratio and
- $m$  = the strength increase exponent.

It should be noted that the calculated yield stress corresponds to the middle of each layer. The undrained strength,  $s_u$ , in Eq. (15) has been derived from CPT test data for the  $N_{kt}$  and  $N_b$  factors values presented in the previous section. The applied  $s_u$  value has been determined at the middle of each layer under consideration after linearization of the undrained shear strength data along the whole length of the layer.

The yield stress values together with the corresponding OCR values for the cross sections 'Raai 1', 'Raai 4' and 'Raai 5' are presented in Table 3.10, Table 3.11 and Table 3.12 respectively. Results for both 'achterland' and 'kruin' locations are shown.

In all of the above tables the sequence of the presented soil layers and the type of the encountered soils is in line with the geological profile of each cross section (Appendix A). For the deepest 'klei-Kreftenheye' layer no parameters have been assessed since laboratory and in situ testing is limited at lower depths. For this layer the soil parameters as derived from previous soil investigation campaign at the same area (KIJK project) are used ( $S_{average} = 0.25$ ,  $m_{average} = 0.8$ ). Reference to the KIJK campaign is given in more detail in section 3.3.



To allow a direct comparison of the OCR values, as these were determined from knowledge of the yield stresses as derived from Eq. (15) with the OCR values calculated experimentally via the performance of Ko-CRS tests an extra column is added in Table 3.10, Table 3.11 and Table 3.12 which present the values of  $OCR_{(Ko-CRS)}$  when these are available. The presented  $OCR_{(Ko-CRS)}$  values do not accurately correspond to the depths of the OCR values calculated in the middle of each layer, nevertheless the difference in depth is not significant.

Location: Kruijn (X=2.5 m_NAP)								
Encountered soil layer	Y (m)_NAP	$\sigma'_v$	$s_u$ (kPa)	$S_{average}(-)$	$m_{average}(-)$	$\sigma_{vc}$ (kPa)	OCR (-)	$OCR_{(Ko-CRS)}$
Klei antropogeen	1.30	42.9	30.7	0.32	0.918	103.0	2.4	-
Klei met schelpen (Echteld)	-1.87	77.3	53.2	0.32	0.918	177.9	2.3	1.7
Klei met plantenresten (Echteld) O1	-4.47	100.6	47.5	0.32	0.918	153.8	1.5	1.7
Hollandveen (Nieuwk)	-5.71	110.3	80.0	0.38	0.881	229.8	2.1	1.7
Klei met plantenresten (Echteld) O2	-8.11	130.6	55.6	0.32	0.918	178.3	1.4	-
Basisveen (Nieuwk)	-10.50	153.6	73.8	0.38	0.881	200.6	1.3	-
Klei (Kreftenheye)	-11.50	165.3	50.2	0.25	0.8	210.8	1.3	-
Location: Achterland (X=13.5 m_NAP)								
Klei antropogeen	-1.20	6.9	79.1	0.32	0.918	17.3	2.5	-
Klei met schelpen (Echteld)	-2.50	17.3	20.3	0.32	0.918	71.1	4.1	2.3
Hollandveen (Nieuwk) N1	-3.98	22.0	17.6	0.38	0.881	51.1	2.3	1.6
Klei met plantenresten (Echteld) N1	-5.28	26.8	12.2	0.32	0.918	39.2	1.5	-
Hollandveen (Nieuwk) N2	-6.25	31.8	29.0	0.38	0.881	85.9	2.7	-
Klei met plantenresten (Echteld) N2	-8.35	44.6	30.8	0.32	0.918	103.1	2.3	-
Basisveen (Nieuwk)	-10.50	56.8	55.5	0.38	0.918	158.8	2.8	-
Klei (Kreftenheye)	-11.50	60.9	39.9	0.25	0.8	203.1	3.3	-

Table 3.10 Yield stress and OCR values for the encountered soils of cross section 'Raai 1'

Location: Kruijn (X=2.5 m_NAP)								
Encountered soil layer	Y (m)_NAP	$\sigma'_v$	$s_u$ (kPa)	$S_{average}(-)$	$m_{average}(-)$	$\sigma_{vc}$ (kPa)	OCR (-)	$OCR_{(Ko-CRS)}$
Klei antropogeen	1.16	27.6	34.9	0.32	0.918	123.3	4.5	1.7
klei met schelpen	-0.66	53.9	38.3	0.32	0.918	128.5	2.4	-
Klei met plantenresten_O1	-2.76	71.9	55.8	0.32	0.918	188.8	2.6	1.5
Klei met plantenresten_O1	-6.36	103.9	61.3	0.32	0.918	202.2	1.9	-
Hollandveen (Nieuwk)_O2	-9.67	129.2	96.3	0.38	0.881	277.6	2.1	-
Klei met plantenresten_O3	-11.91	155.3	59.1	0.32	0.918	187.4	1.2	-
Location: Achterland (X=15.5 m_NAP)								
Klei met schelpen (Echteld)	-2.88	11.3	7.7	0.32	0.918	25.6	2.3	-
Klei met plantenresten (Echteld)_N1	-4.00	20.0	16.7	0.32	0.918	56.9	2.8	2.1
Hollandveen (Nieuwk)_N1	-5.04	27.4	20.7	0.38	0.881	59.6	2.2	-
Klei met plantenresten (Echteld)_N2	-5.95	33.7	23.1	0.32	0.918	77.4	2.3	-
hollandveen (Nieuwk)_N2	-8.73	45.7	25.9	0.38	0.881	71.9	1.6	1.3
Klei met plantenresten (Echteld)_N3	-11.90	65.2	21.7	0.32	0.918	68.1	1.0	-

Table 3.11 Yield stress and OCR values for the encountered soils of cross section 'Raai 4'

Location: Kruijn (X=2.5 m_NAP)								
Encountered soil layer	Y (m)_NAP	$\sigma'_v$	$s_u$ (kPa)	$S_{average}(-)$	$m_{average}(-)$	$\sigma_{vc}$ (kPa)	OCR (-)	$OCR_{(Ko-CRS)}$
Klei antropogeen	0.96	31.2	43.1	0.32	0.918	153.6	4.9	-
Klei met schelpen (Echteld)	-1.57	63.1	59.0	0.32	0.918	203.0	3.2	1.7
Hollandveen (Nieuwk)_O1	-2.51	62.9	54.5	0.38	0.881	160.3	2.5	-
Klei met plantenresten (Echteld)	-2.92	63.9	49.6	0.32	0.918	167.7	2.6	-
Hollandveen (Nieuwk)_O2	-5.15	87.5	63.7	0.38	0.881	183.1	2.1	1.5
Klei met plantenresten (Echteld)	-7.77	120.6	50.2	0.32	0.918	160.8	1.3	-
Location: Achterland (X=12.7 m_NAP)								
Klei met schelpen (Echteld)	-2.62	21.1	26.9	0.32	0.918	95.0	4.5	-
Klei met plantenresten (Echteld)_N1	-3.15	28.7	31.8	0.32	0.918	111.0	3.9	3.3
Hollandveen (Nieuwk)_N2	-5.27	33.9	22.8	0.38	0.881	64.9	1.9	1.4
Klei met plantenresten (Echteld)_N2	-8.20	50.6	22.6	0.32	0.918	72.7	1.4	-

Table 3.12 Yield stress and OCR values for the encountered soils of cross section 'Raai 5'

The uncertainty in the calculation of the yield stress values depends on the uncertainties in the calculations of  $S$ ,  $m$  and  $N_{kt}/N_b$  values with the latter having the major impact (Duncan, 2000). The coefficient of variation for the uncertainty in the calculation of yield stress is taken to be 85% of the coefficient of variation of the  $N_{kt}/N_b$  following the WBI (2017) recommendations. The computed coefficients of variation for the uncertainty in the calculation of yield stress are summarized in Table 3.13 below.

Type of soil	Kruin: VC [-]	Achterland: VC [-]
Clay	0.18	0.18
Peat	0.18	0.11

Table 3.13 Coefficients of variation for the uncertainty in the calculation of yield stress

### 3.3 Comparison with data from previous soil investigation campaign (KIJK Project)

In this Section of the report the soil parameters as assessed in a previous soil investigation campaign along the river Hollandse IJssel are compared with the findings of current survey. The previous campaign was carried out by Fugro and Royal HaskoningDHV for the purposes of the KIJK project (Krachtige IJsseldijken Krimpenerwaard) commissioned by the Hoogheemraadschap van Schieland and the Krimpenerwaard.

The average, characteristic and design soil parameter values as used in the calculations for the KIJK project are summarized and presented in Table 3.14, Table 3.15 and Table 3.16 (Royal HaskoningDHV, 2016-1).

To facilitate a direct comparison the above tables also present the corresponding parameter values as these were derived in current project. In regards to the values from this study it should be noted that:

- In situ and laboratory testing is limited to cohesive layers. As a result, no data are available for the encountered sand layers. For the purpose of this project a distinction is made among a 'zand, antropogeen' and a 'zand, kreftenheye' layer. Considering a loose density state an average and a characteristic value of  $\varphi' = 32.5^{\circ}$  and  $30^{\circ}$  respectively is adopted for the 'zand, antropogeen' following NEN recommendations. Considering a medium dense state the corresponding values for the 'zand, kreftenheye' layer are  $\varphi' = 35^{\circ}$  and  $32.5^{\circ}$ . For the determination of the design values the characteristic  $\tan(\varphi')$  values of the above layers are divided by a material factor  $\gamma_m = 1.06$  as this factor is given in OI2014v3.
- Laboratory testing data are not available for the 'Klei Kreftenheye' layer. Thus, a direct comparison of the soil parameter values of this layer with the ones from Kijk project is not feasible. For this layer the soil parameters  $S$  and  $m$  as assessed in the Kijk campaign have been adopted.
- The design values for the  $m$  parameter are determined both for the peat and clay layer by dividing the characteristic  $m$  values with a material factor of  $\gamma_m = 1.00$ . The same procedure has been applied for the determination of the design  $S$  ratio values. However for this case a material factor of  $\gamma_m = 1.07$ ,  $\gamma_m = 1.04$ ,  $\gamma_m = 1.18$  and  $\gamma_m = 1.05$  is applied for 'klei, antropogeen', 'klei, met schelpen', 'klei met plantenresten' and 'Hollandveen'

layer respectively. The selected material factor values are in accordance with the values recommended in OI2014v3.

- For the determination of the design  $\phi'$  values the characteristic  $\tan(\phi')$  values for the clay and peat layers have been divided by a material factor  $\gamma_m = 1.20$  and  $\gamma_m = 1.25$  respectively. For the determination of the design  $c'$  values the characteristic  $c'$  values for the clay and peat layers have been divided by material factor  $\gamma_m = 1.25$  and  $\gamma_m = 1.50$  respectively. The aforementioned material factors' values are in accordance with the values given in ATRWG.
- The presented  $\phi'$  and  $c'$  values (average, characteristic and design) correspond to large strains (25% axial strain for clay samples and 40% shear strain for peat samples).
- It should be noted that the naming of the clay layers in the KIJK and POVM project is not consistent. This could be accounted to the use of different guidelines for soil description and classification and to their interpretation from the person providing the descriptions. In the POV-M project the samples were classified according to NEN 5104.

KIJK PROJECT								POV-M PROJECT								
Type of soil	$N_{kt, gem}$		$m_{gem}$		POP <sub>gem</sub> [kPa]		$S_{gem}$ [-]	$\phi_{gem}^{[0]}$	$C'_{gem}$ [kPa]	Type of soil	$N_{kt, gem}$	$N_{b, gem}$	$m_{gem}$	$S_{gem}$	$\phi_{gem}^{[0]}$	$C'_{gem}$
	Teen	[-]	Kruin	Teen	Kruin	Teen					Kruin	Teen	[-]	[-]	[ $^{\circ}$ ]	[kPa]
Veen	20.1	0.83	85	42	0.55	-	-	Hollandveen	15.7	14.71	0.88	0.38	29.3	7.48		
Detritus	20.1	0.87	68	43	0.33	-	-									
Gyttja	20.1	0.88	57	42	0.34	-	-									
Veen, kleilig	20.1	0.85	99	40	0.4	-	-									
Klei antropogeen	NA	0.9	54	41	0.43	-	-	Klei met schelpen	15.33	14.55	0.92	0.32	31.3	7.32		
Klei humeus	17.5	0.87	54	38	0.33	-	-	Klei met plantenresten								
Klei siltig	17.5	0.89	71	40	0.31	-	-	Klei antropogeen								
Klei kreftenheye	20	0.8	25	25	0.25	-	-	Klei kreftenheye	-	-	0.8	0.25	-	-		
Zand	-	-	-	-	-	NA	0	Zand antropogeen	-	-	-	-	32.5	0		
								Zand kreftenheye	-	-	-	-	35	0		

Table 3.14 Comparison of mean soil parameters values; KIJK – POV-M project

KIJK PROJECT								POV-M PROJECT								
Type of soil	$N_{kt, kar}$		$m_{kar}$		POP <sub>kar</sub> [kPa]		$S_{kar}$ [-]	$\phi_{gem}^{[0]}$	$C'_{kar}$ [kPa]	Type of soil	$N_{kt, kar}$	$N_{b, kar}$	$m_{kar}$	$S_{kar}$	$\phi_{gem}^{[0]}$	$C'_{kar}$
	Teen	[-]	Kruin	Teen	Kruin	Teen					Kruin	Teen	[-]	[-]	[ $^{\circ}$ ]	[kPa]
Veen	NA	0.77	NA	NA	0.36	-	-	Hollandveen	-	-	0.86	0.36	28.4	0.41		
Detritus	NA	0.86	NA	NA	0.27	-	-									
Gyttja	NA	0.88	NA	NA	0.27	-	-									
Veen, kleilig	NA	0.83	NA	NA	0.35	-	-									
Klei antropogeen	NA	0.87	NA	NA	0.31	-	-	Klei met schelpen	-	-	0.89	0.29	31.3	0*		
Klei humeus	NA	0.85	NA	NA	0.30	-	-	Klei met plantenresten								
Klei siltig	NA	0.87	NA	NA	0.27	-	-	Klei antropogeen								
Klei kreftenheye	NA	0.73	NA	NA	0.21	-	-	klei kreftenheye	-	-	0.73	0.21	-	-		
Zand	-	-	-	-	-	32	0	Zand antropogeen	-	-	-	-	30	0		
								Zand kreftenheye	-	-	-	-	32.5	0		

\*The  $c'_{kar}$  value is taken equal to 2 kPa when lognormal distribution is considered.

Table 3.15 Comparison of characteristic soil parameters values; KIJK – POV-M project

KIJK PROJECT								POV-M PROJECT						
Type of soil	$N_{kt,d}$	$m_d$ [-]	$POP_d$ [kPa]		$S_d$ [-]	$\phi_{gem}$ [°]	$C'_d$ [kPa]	Type of soil	$N_{kt,d}$	$N_{b,d}$	$m_d$ [-]	$S_d$ [-]	$\phi_{gem}$ [°]	$C'_d$ [kPa]
	Teen		Kruin	Teen					Kruin	Teen				
Veen	NA	0.73	NA	NA	0.34	-	-	Hollandveen	-	-	0.86	0.34	23.4	0.27
Detritus	NA	0.82	NA	NA	0.25	-	-							
Gyttja	NA	0.82	NA	NA	0.26	-	-							
Veen, kleilig	NA	0.79	NA	NA	0.30	-	-							
Klei antropogeen	NA	0.83	NA	NA	0.29	-	-	Klei met schelpen	-	-	0.89	0.28	26.9	0
Klei humeus	NA	0.81	NA	NA	0.26	-	-	Klei met plantenresten				0.25		
Klei siltig	NA	0.83	NA	NA	0.26	-	-	Klei antropogeen				0.27		
Klei kreftenheye	NA	0.7	NA	NA	0.20	-	-	Klei kreftenheye				0.7		
Zand	-	-	-	-	-	27.5	0	Zand antropogeen	-	-	-	-	28.6	0
								Zand kreftenheye	-	-	-	-	31	0

Table 3.16 Comparison of design soil parameters values; KIJK – POV-M project

## 4 Summary and Conclusions

An extensive testing program which consisted of in situ and advanced laboratory tests was performed on the subsoil from the dike's sections along the river Hollandse IJssel with one of the objectives to obtain the soil parameters required in FEM and LEM calculations. This report summarizes and presents the derived parameter values while it describes the procedures, guidelines and formulas applied for their computation.

Additional aspects of the testing program included investigation on the influence of the direction of loading on the undrained shear strength properties of soil via the performance of conventional DSS and Large DSS (LDSS) tests with the direction of shearing applied parallel or perpendicular to the dike. The test results from both types of tests reveal that the undrained shear strength of the samples remains unaffected by the direction of loading. This finding implies that the stress history of the peat tested in this study in terms of pre-shearing in a predominant direction does not influence the undrained shear strength response when shearing of the soil takes place in a different direction to the pre-shearing one.

The impact of scale on the direct simple shear testing of the encountered peat layers has also been assessed via the performance of conventional DSS and large scale DSS (LDSS) tests on samples retrieved from adjacent locations and tested at similar depths. Unfortunately, the tested material appeared to be different from material that was tested by the conventional DSS tests. To fully benefit from the positive results of the LDSS tests it is recommended to do additional tests on newly retrieved samples.

A comparison of design values for the different strength parameters as assessed in current study with the ones from a previous investigation campaign within the same area of interest (KIJK project) is provided. The reported parameter values among the two projects do not differ significantly. The POV-M parameters have been derived based on an extensive test results database on specific cross sections while the parameters for the KIJK project have a wider spread in the area of investigation.



## 5 References

- Hoffmans, G. (2007). ATRWG: Addendum bij het technisch rapport waterkerende grondconstructies.
- Calle, E and Alexander van Duinen (2016). Bepaling karakteristieke waarden schuifsterkte parameters. Deltares memo 1220132-003-GEO-0002.
- Den Haan E.J. Grognet M (2014) A large direct simple shear device for testing peat at low stresses Géotechnique letters no 4 p 283-288.
- Wood, D. (1990). Soil behaviour and critical state soil mechanics. Cambridge University Press, Cambridge.
- Den Haan E.J., Kamao S. (2003). Obtaining isotache parameters from a CRS K0 oedometer Soils and Foundations vol 43. no 4 p 203-214
- Duncan, J.M. (2000). Factors of Safety and Reliability In Geotechnical Engineering. J. Geotech. Geoenviron. Eng. 2000.126:307-316.
- OI (2015). Handreiking ontwerpen met overstromingskansen, Veiligheidsfactoren en belastingen bij nieuwe overstromingsnormen. Report Concept vs. 2.5, Rijkswaterstaat Water, Verkeer en Leefomgeving.
- RoyalHaskoningDHV (2016-1). Rapport Consequentieanalyse Krachtige IJsseldijken Krimpenerwaard, Referentie: WATBE2432R002F02, Versie: 02/Finale versie, Datum: 13 Mei 2016.
- Seah, T.H., Lai, K.C. (2003). Strength and deformation behavior of soft bangkok clay. Geotechnical Testing Journal, 26(4), 421–431.
- Technische Adviescommissie voor de Waterkeringen (2001). Technisch Rapport Waterkerende Grondconstructies.
- Termaat, R.J., Vermeer, P.A., Vergeer, C.J.H. (1985). Failure by large plastic deformations. In Proceedings of the 11th International Conference on Soil Mechanics and Foundation Engineering, San Francisco, 12-16 Aug.
- WBI (2017). Schematiseringshandleiding macrostabiliteit. Datum: 1 September 2016.
- Wiertsema and Partners (2016). Geotechnisch onderzoek. Grondonderzoek POVM 'Beter benutten actuele sterkte' te Krimpen aan den IJssel, VN-63788-1, 29 Juli 2016.
- Zwanenburg C. , Van M.A. (2015) Comparison between conventional and large scale triaxial compression tests on peat 15<sup>th</sup> Pan American Conference on Soil Mechanics and Geotechnical Engineering Buenos Aires.



## **A Geological profile of cross sections**





## **B Computation of field effective stress level**



## **C CAU test results**



## **D DSS test results**



## **E K<sub>0</sub>-CRS results**



## **F Large DSS results**



## **G Atterberg limit results**



## **H PSD test results**



## I Classification test results